ALMA MATER STUDIORUM
UNIVERSITÀ DI BOLOGNA

DEPARTMENT OF INDUSTRIAL ENGINEERING

SECOND CYCLE DEGREE IN

MECHANICAL ENGINEERING FOR SUSTAINABILITY

SHEET MOLDING COMPOUND APPLICATIONS FOR ORIGAMI-INSPIRED METAMATERIALS

Supervisor

Prof. Lorenzo Donati

Co-Supervisor

Prof. Sara Bagassi

Co-Supervisor

Eng. Martino Carlo Moruzzi

Defended by

Houssein Mhanna

Academic Year 2024/2025

To my uncle Anderson, who inspired me to dream and persevere.

To my brother Mohammad, my constant source of strength and encouragement.

And to my parents Ayyad and Rose, for their endless love and sacrifices.

Abstract

This thesis explores a low-cost, scalable manufacturing approach for an origami-inspired acoustic metamaterial by combining forged short-fiber carbon-epoxy composites with 3D-printed polymer molds. A Miura-Ori-based unit cell was chosen for its acoustic characteristics, and a complete workflow was developed: CAD modeling of the unit cell, design of multi-part molds for FDM production, iterative forging with chopped 6K carbon fibers and a room-temperature IN2 epoxy/AT30 hardener system, mechanical characterization, and a four-unit-cell scale-up demonstration. The process was refined across three iterations to address voids, fiber gaps, and compaction issues. The optimized procedure produced defect-free tensile test specimens that exhibited a predominantly linear elastic response in tensile testing. Results were benchmarked against Aluminum 5154-H36 specimens produced under the same test conditions, showing that the forged composite provides a favorable stiffness-to-weight ratio for non-primary aerospace components. A four-cell component was successfully fabricated confirming scalability; minor defects observed in the multi-cell part were traced to pressure distribution and are addressable. The study demonstrates that 3D-printed molds and forged carbon-fiber processing represent a viable route for producing complex metamaterial geometries, offering rapid iteration, reduced tooling cost, and acceptable mechanical performance for applications such as acoustic inserts and interior aircraft panels.

Acknowledgements

First and foremost, I would like to express my gratitude to my supervisor, Lorenzo Donati, Full Professor at the Department of Industrial Engineering of the University of Bologna, as well as my assistant supervisors, Sara Bagassi, Associate Professor at the Department of Industrial Engineering of the University of Bologna, and Martino Carlo Moruzzi, Research Fellow at the Department of Industrial Engineering of the University of Bologna. Their guidance, resources and assistance were instrumental in the completion of this dissertation.

I would also like to give special thanks to both, Paolo Proli, Technical Manager of laboratory units supporting teaching and/or research at the Department of Industrial Engineering of the University of Bologna, Lorenzo Magnani, PhD Student at the Department of Industrial Engineering of the University of Bologna. Their practical support and technical expertise were fundamental during the experimental phases of this work and greatly contributed to the successful realization of this thesis.

In addition, I would like to express my appreciation to the M.Sc. Mechanical Engineering for Sustainability degree program board, as well as the faculty staff. Also, I would like to thank my professors for giving me the opportunity of studying abroad, helping me enhance my academic knowledge and providing insight in the mechanical sector.

Last but not least, I would like to express my immense gratitude to my family, for their inspiration, encouragement and unparalleled support, as well as my friends, back home and here in Italy for being there through it all. Finally, I would like to thank my colleagues, for their social support and assistance throughout the duration of this program.

Contents

List of Figures

List of Tables

Introduction

Additive manufacturing and modern composite processing are enabling new design paradigms that combine complex geometry with advanced material performance. This thesis investigates a manufacturing route for producing an origami-inspired acoustic metamaterial by combining forged short-fiber carbon composites with low-cost, additively manufactured molds. The work aims to demonstrate that 3D-printed polymer molds can be used as practical tooling for compression forging of discontinuous carbon-fiber composites, enabling rapid iteration and scalability for engineered acoustic metamaterials.

The specific objectives of the research are: (1) to design and produce a complex Miura-Ori-based unit cell using CAD and 3D-printed molds; (2) to develop and optimize a forged carbon-fiber (FCF) manufacturing procedure compatible with polymer tooling; (3) to characterize the mechanical performance of the optimized composite and compare it to an aluminum benchmark; and (4) to validate process scalability by building a multi-cell component. The methodology combines CAD-based mold design, FDM mold fabrication, iterative process optimization (three experimental iterations), mechanical tensile testing under ASTM standards, and a four-unit-cell scalability demonstration.

The structure of the thesis follows this logic. Chapter 1 introduces additive manufacturing with a focus on FDM and tooling applications. Chapter 2 reviews composite materials, with emphasis on short-fiber forgings and matrix selection. Chapter 3 details the design and manufacturing procedures: CAD design of the unit cell and mold, material selection, printing and post-processing of molds, and the experimental steps used to produce the specimens. Chapter 4 presents the experimental results—including defect analysis, process refinements, mechanical testing, and the scalability study—and discusses implications for manufacturability and application. The thesis concludes with a summary of findings, an evaluation of the method's applicability for aerospace and acoustic applications, and recommendations for further work.

Chapter 1

Additive Manufacturing

1.1 Introduction

This chapter introduces the concept of Additive Manufacturing (AM) as one of the most transformative technologies in modern engineering and product development. The objective is to provide a comprehensive understanding of the principles, methodologies, and applications of AM, establishing the foundation for its later use in this thesis.

The chapter begins with a definition of additive manufacturing, describing its fundamental working principles and differentiating it from traditional subtractive techniques. Within this section, special attention is given to the role of Computer-Aided Design (CAD), which serves as the digital backbone of every additive process, enabling precise geometry control and design flexibility.

The discussion then progresses to Rapid Prototyping, outlining how AM technologies have revolutionized the development of functional prototypes. The related concept of Rapid Tooling is introduced as an extension of rapid prototyping, emphasizing how additive processes can produce not only final parts but also functional tools and molds. A dedicated subsection further explores the use of 3D-printed molds, highlighting their advantages in reducing cost, lead time, and material waste—key motivations behind their selection in this research.

Finally, the chapter reviews the main additive manufacturing processes, classifying them according to their material deposition. Particular emphasis is placed on Fused Deposition Modeling (FDM), as it represents the specific process employed in this study for fabricating the experimental molds.

1.2 Definition

Additive manufacturing is a combination of manufacturing methods where a three-dimensional physical object is created using digital schematics like Computer Aided Design or three-dimensional models, or as defined by ASTM, additive manufacturing is a process of joining materials to make parts from 3D model data, usually layer upon layer, as opposed to subtractive manufacturing and formative manufacturing methodologies [1]. It is considered an advanced manufacturing technique used for complex geometries and structures where materials are blended using fusion, binding or solidifying. There are many methods for additive manufacturing such as Fused Deposition Modeling, Stereo Lithography (SLA), Selective Laser Sintering (SLS) and many other methods that differ by the type of deposition or their materials. These methods have gotten a lot of traction and interest in the latest years of production and manufacturing of materials and products. As of now, they are still a novel concept mainly used for academic purposes, but the evolving of the technology has started to bear fruit as there have been implementations in low volume productions processes or for the creation of low-cost prototypes [2, 3].

1.2.1 Computer Aided Design (CAD)

CAD is the usage of computer systems in order to aid in the creation, analysis and modification of a design. Usually, for typical applications, Computer Aided Design consists of a software suite of Graphical User Interface (GUI), able to perform the design functions [4].

Using the functions of the software, the user is able to design both two-dimensional and three-dimensional shapes with various sizes and geometries, in order to create the desired final geometry. The functions used in this software are preprogrammed to facilitate the geometric or mechanical requirements desired by the user. These applications are able to perform test on the design such as stress-strain analysis, dynamic response, heat transfer simulation and much more.

CAD serves as the basic starting point for any additive manufacturing process, as it creates the intended geometry to be manufactured.

1.3 Rapid Prototyping

Rapid Prototyping was introduced in the 1980s as one of the first Additive Manufacturing processes. It is a generic term that refers to a number of technologies and processes that generate a three-dimensional geometry in a quick manner, without the need for conventional tooling or skilled machinists. The technology works by depositing a material layer by layer until you reach the final geometry, using CAD as a basis. The main advantages shown are the construction of high complexity structures, which could be very hard to make using typical subtractive manufacturing methods, with a significant reduction in the time required. The method of layer deposition and material used vary depending on the properties desired of the final part [5].

The method of Rapid Prototyping works in a manner of firstly designing the required geometry and transforming it to a format that the slicer can read, usually STL. A slicer is an external software which transforms the geometry into a toolpath that the machine can perform, and STL is a standard template that describes the geometry using triangles [6]. After preparing the toolpath, the slicer exports a format that the machine can read. Afterwards, the machine performs two dimensional movements to create one layer of material, then it changes the elevation to do another layer and it keeps repeating this process until the desired geometry is reached.

The process of rapid manufacturing was made possible by the prior introduction of CAD, computer aided manufacturing (CAM) and computer numerical control (CNC). The integration of these technologies over time made it possible to produce three-dimensional geometries for commercial applications. In addition to the reduced limitations regarding geometric complexity, the user-friendly nature of these systems for both professionals and hobbyists represents a significant market advantage. The process framework is illustrated in Figure 1.

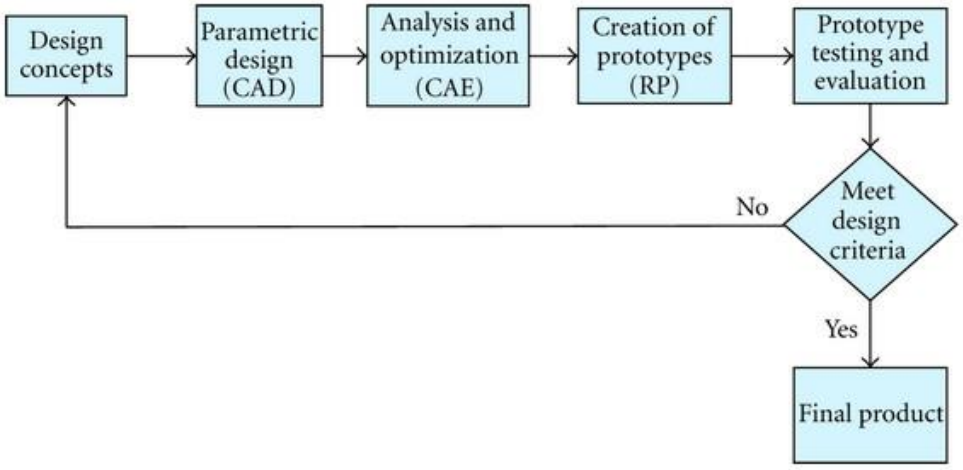

Figure 1 Development of rapid prototyping model [7].

At the present time, the technologies of rapid prototyping are not just used for creating models, with the advantages in plastic materials it has been possible to create finished products, of course at the beginning they were developed to expand the situations tested in the prototyping process. Nowadays, these technologies have other names like 3D printing, and so forth, but they all have the origins of rapid prototyping. This process is sometimes referred to as 2.5D printing and not 3D printing because it is a repeated two-dimensional action [8]. According to Wohler's report 2011 the growth rate for 2010 was 24.1%. The compound annual growth rate for the industry's history, until 2010, is 26.2% [9]. This growth is shown in Figure 2.

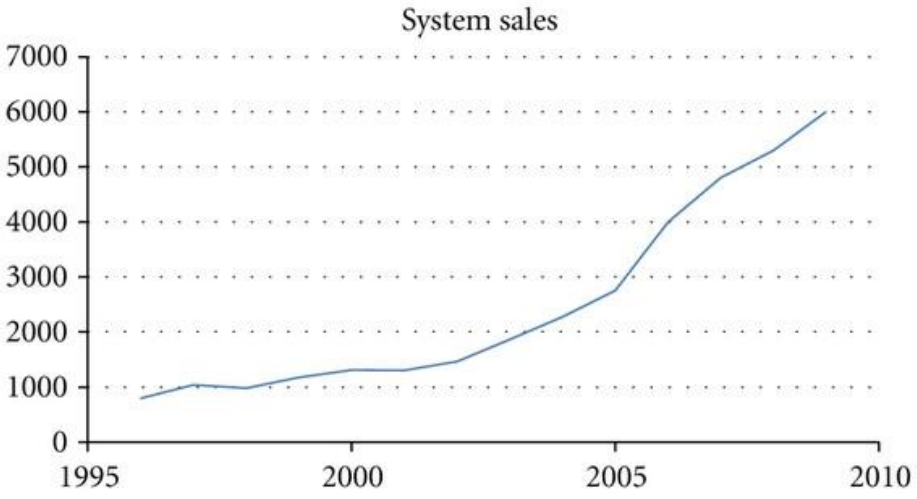

Figure 2 Growth of rapid prototyping [10].

1.3.1Rapid Tooling

Rapid Tooling is an advancement of Rapid Prototyping, focusing on the fast production of molds or tools used for creating final components. Similar to Rapid Prototyping, it offers significant advantages in cost and lead time compared to conventional subtractive manufacturing methods traditionally used to produce tooling.

There are two main approaches to Rapid Tooling: direct and indirect. In direct rapid tooling, the tool itself is produced directly through AM and can be used immediately for forming or molding processes. In indirect rapid tooling, an AM-produced model serves as a master pattern or mold, which is then used to create the final tool from another material through casting or molding techniques.

Rapid Tooling methods can also be classified based on the material used for tool fabrication, with the most common being polymers, metals, and ceramics. Polymer-based tooling is often preferred in prototyping and low-volume production, due to its lower cost and ease of processing, while metal tooling is used when higher durability or temperature resistance is required.

An important distinction between Rapid Tooling and Rapid Prototyping lies in the design considerations required. Unlike prototypes, tools must account for manufacturing factors such as draft angles, shrinkage allowance, thermal expansion, and surface finish, which directly influence the accuracy and quality of the parts produced.

Overall, Rapid Tooling serves as a bridge between rapid prototyping and full-scale production, enabling faster design validation, reduced manufacturing time, and greater flexibility in producing complex geometries [11].

1.3.2 3D Printed Molds

In recent scientific literature, only a limited number of studies have focused on the application of AM for mold fabrication. For instance, the integration of AM with conventional casting techniques has enabled the development of hybrid molding processes for simultaneously producing sand molds and sand cores [12].

Yang et al. [13] introduced an innovative approach to manufacturing frozen sand molds using water as a binder instead of traditional resin-based binders, specifically for low-temperature additive manufacturing environments. Their study examined the liquid–solid phase transition mechanism of the binder, as well as the temperature field variations and phase transition behavior within a pre-cooled powder bed. From these investigations, the process window for frozen sand mold fabrication was established, presenting a novel and environmentally friendly casting technique for the foundry industry. Kim et al. [14] explored the feasibility of applying a thermoset polymer surface coating onto additively manufactured carbon fiber-reinforced polyphenylene sulfide (CF-PPS) composite molds. The thermal stability of the coating was evaluated over multiple heating cycles, showing no significant thermal degradation. Pull-off adhesion tests conducted after repeated thermal cycling indicated no notable reduction in adhesion strength, even after ten cycles. Similarly, Hassen et al. [15] presented a method for fabricating polymer molds using additive manufacturing in segmented sections with an O-ring joint design. These molds could be machined and assembled for use in autoclave environments. Across a temperature range of 20–200 °C, the multi-part mold design maintained full vacuum conditions (~73.7 cmHg) with minimal leakage (<1.5 cmHg/5 min). Despite these advancements, there remains a notable scarcity of research dedicated to the use of additive manufacturing for mold production.

Traditional mold fabrication, typically carried out using metals such as steel or aluminum, is a highly demanding and resource-intensive process. The manufacturing of metal molds requires precision machining operations, including milling, drilling, and surface finishing, all of which contribute to long lead times and elevated production costs. Moreover, due to the high cost of both raw materials and machining labor, any design error or modification during fabrication can result in significant financial loss and wasted material, making the process inefficient for iterative development. The complexity increases further when intricate geometries or fine surface details are required, as additional tooling and specialized equipment are often needed.

In contrast, additive manufacturing enables the creation of molds through 3D printing, offering substantial advantages in terms of flexibility, cost, and time efficiency an example is shown in Figure 3. The digital workflow allows rapid adjustments to the mold design, minimizing the impact of design changes and eliminating the need for extensive re-machining. The ability to produce complex geometries without additional tooling further enhances design freedom and accelerates the prototyping process. For research and small-scale production, where only a limited number of parts are needed, 3D-printed molds represent a highly practical and economical alternative to traditional metal molds, as they reduce both lead time and material waste.

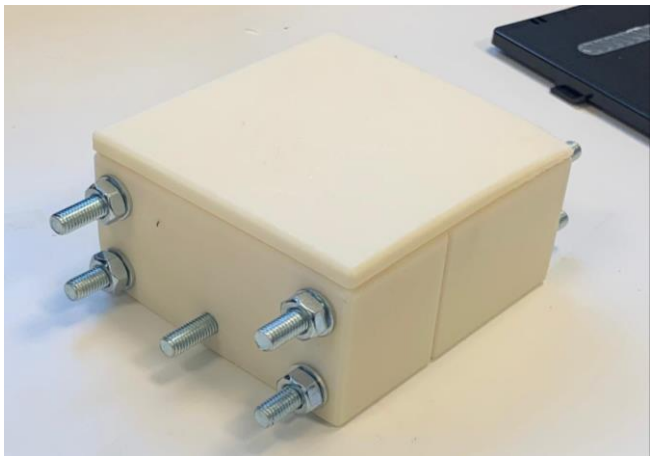

Figure 3 Mold made with additive manufacturing technology.

From a sustainability perspective, the use of polymer-based 3D-printed molds also aligns with environmentally conscious manufacturing practices. Additive processes inherently minimize material waste by depositing only the necessary amount of material, while many thermoplastic filaments can be recycled or reprocessed. Furthermore, the reduced energy consumption and shorter production cycles contribute to a lower overall environmental footprint. Consequently, 3D-printed molds not only provide a cost-effective and flexible solution but also support sustainable manufacturing approaches, making them particularly suitable for experimental studies and rapid prototyping applications.

Despite the clear advantages of 3D-printed molds in terms of cost, flexibility, and sustainability, certain limitations must be acknowledged when compared to conventional metal molds. One of the primary concerns lies in the significantly lower thermal conductivity of polymer-based molds, such as those made from ABS or PETG. Metals like aluminum and steel dissipate heat efficiently, allowing for uniform temperature distribution during curing or forming processes. In contrast,

thermoplastic molds tend to retain heat, which can lead to uneven curing of composite materials and longer cooling times.

Additionally, mechanical strength and dimensional stability are generally inferior in 3D-printed polymers compared to metals, especially under elevated temperatures or mechanical loads. This may restrict their use to low-pressure forming processes or short production runs. Nevertheless, through careful design optimization, post-processing, and material selection, these limitations can be mitigated to a considerable extent. Consequently, while polymer molds may not yet fully replace metal ones in high-volume or high-temperature applications, they remain a highly viable option for prototyping, experimental studies, and low-volume production.

1.4 Additive Manufacturing Printing Processes

The earliest additive manufacturing technique, STL, was introduced in the late 1980s. Since then, numerous other methods have been developed for a variety of materials such as plastics and metals, each employing distinct printing techniques and strategies, and offering different levels of precision and material properties. Figure 4 provides an overview of the various additive manufacturing processes.

The method used in this thesis is FDM. Consequently, a brief explanation of slurry-based additive manufacturing methods should be included. Slurry based methods are the additive manufacturing systems considered as a sub-category of liquid based methods, where a semi-liquid or paste-like material is spread or extruded layer by layer onto a build surface, and each layer is subsequently solidified through drying, sintering or curing processes. These methods are commonly employed for plastic, ceramic, metal, or composite materials, where achieving a high particle concentration within the slurry allows for dense and mechanically robust final parts [16].

Additive manufacturing technologies are classified by materials as: liquid based, solid based, slurry based and powder Based. Liquid based methods including Stereolithography (SL) and PolyJet, use photopolymer resins that solidify through light-induced polymerization. Slurry based methods include materials in a viscous form like Binder Jetting or filament form like Fused Deposition Modeling. Solid-based methods, such as Laminated Object Manufacturing (LOM), use solid sheets that are cut and bonded to form the part. Powder-based methods use powdered materials that are fused or bound together, with melting techniques like SLS, EBM, and LENS [17].

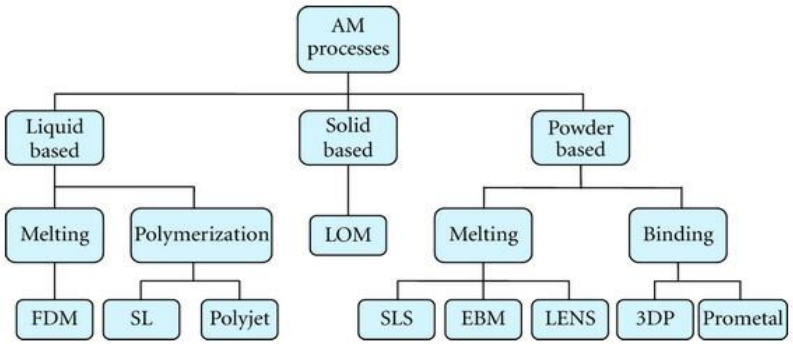

Figure 4 Three-Dimensional printing processes [18].

1.4.1 Fused Deposition Modelling (FDM)

For our application, as will be mentioned in Section 3.2, a printer which utilizes the FDM printing method was operated, so this is the additive manufacturing technology of interest.

Fused deposition modelling is a method of additive manufacturing that was developed in the late 1980s and is one of the most widely distributed filament-based methods, its illustrated in Figure 5. In this method, a thin plastic spool of filament is fed to a printing head. There, the material is heated up to melting point and extruded into the printing surface through a nozzle, forming the desired surface with the pre-selected printing pattern. The head moves on X and Y axis, in order to deposit material and form the desired surface layer. When one layer is cooled out and solidified, the head moves upwards along the Z-axis, and starts depositing material and another layer is formed, as specified by the design provided. With this iterative procedure, layer-by-layer, the 3D printer is able to generate the desired geometry. In addition, a secondary material is melted and extruded to provide support during the printing process. Usually, the first few layers of the print are a supporting printing base built

out of the support material, in order to keep the material in position, also known as Raft. This support material has the advantage of being soluble, so that the combined structure can easily dissolve, and the only part left is the structure made out of the main filament [7].

The printing pattern plays a crucial role as it influences the density of the printed geometry, which in turn affects the overall printing time, filament consumption, and the mechanical characteristics of the final component, such as tensile strength. Common materials used in the deposition process include Polycarbonate (PC), Acrylonitrile Butadiene Styrene (ABS), Thermoplastic Polyurethane (TPU), Polylactic Acid (PLA), PC-ABS blends, and PC-ISO—the latter primarily utilized in medical applications.

One of the main advantages of FDM is that it does not require much post-processing or resin curing. Additionally, both the equipment and materials are relatively inexpensive, making it a highly cost-efficient technique. Nevertheless, there are some limitations: the resolution along the Z-axis is lower compared to other additive manufacturing technologies, often necessitating post-processing to improve surface finish. Furthermore, the process can be quite slow, sometimes taking several days to complete a single geometry.

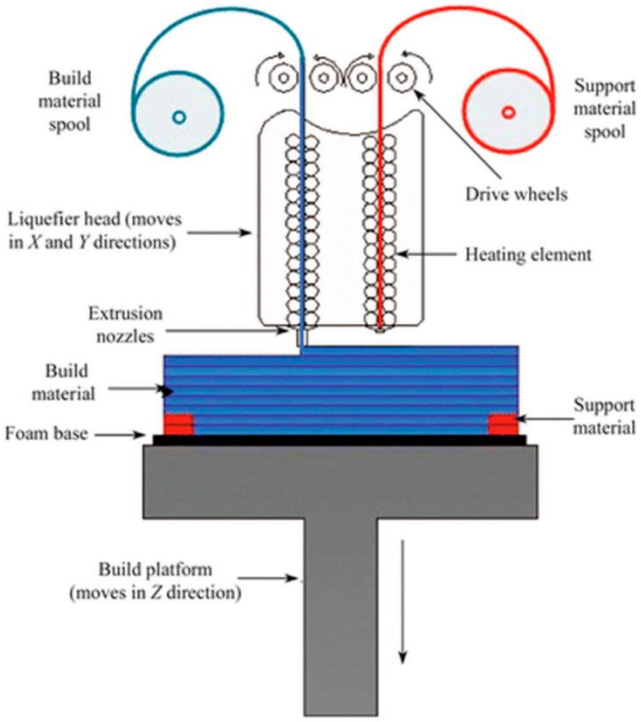

Figure 5 FDM technology scheme [19].

As will be discussed later in section 3.2, the Stratasys Fortus 250mc supports two materials: ABSplus as the primary filament and SR-30 as the support material. Acrylonitrile Butadiene Styrene (ABS) is a thermoplastic polymer with an amorphous structure composed of the three monomers mentioned above. Since the printer uses proprietary cartridges supplied by the manufacturer, these are the only materials compatible with the system. When the monomers combine, they form two co-polymer phases that make up the ABS material. The combination of the strength and rigidity of acrylonitrile and styrene with the toughness of polybutadiene results in a well-balanced set of mechanical properties. The specific ratio of each monomer directly influences the final part's mechanical performance. ABS is widely utilized in additive manufacturing, particularly in FDM processes.

However, the primary focus of this thesis will be on the use of ABS molds in the manufacturing of Forged Carbon Fiber components. The ABS molds serve as a formwork to shape the composite material during the compression and curing process. Unlike typical metal molds, ABS molds have not been studied as excessively. Studying the durability and reusability of the molds is essential, as repeated use may affect the surface quality and dimensional accuracy of the final parts. Additionally, the mechanical properties of the Forged Carbon Fiber components will be evaluated to assess the effectiveness of the ABS mold in preserving the intended geometry and structural performance. By investigating both mold performance and the properties of the final composite, this research aims to provide a comprehensive understanding of the potential and limitations of ABS molds in advanced composite manufacturing.

Chapter 2

Composite Materials

2.1 Introduction

This chapter provides an overview of composite materials, focusing on their composition, classification, manufacturing methods, and engineering applications. The aim is to establish the theoretical background required to understand the material behavior and performance of the Forged Carbon Fiber composite developed in this study.

The chapter begins by defining composite materials and describing their fundamental concept as a combination of two or more distinct phases—typically a reinforcing phase and a matrix phase—that together yield superior properties compared to their individual constituents. The classification of composites is briefly discussed based on reinforcement type (fibers, particles, or laminates) and matrix nature (polymer, metal, or ceramic).

Subsequent sections explore the mechanical and physical characteristics of fiber-reinforced composites, with an emphasis on the influence of fiber length, orientation, and volume fraction on stiffness, strength, and overall performance. Special attention is given to carbon fiber composites, which are known for their exceptional strength-to-weight ratio, dimensional stability, and thermal resistance—qualities that make them ideal for aerospace and advanced structural applications.

The discussion then covers the manufacturing methods used in composite production, including traditional techniques such as hand lay-up, vacuum infusion, and compression molding, as well as modern approaches like Forged Carbon Fiber (FCF). This emerging process combines chopped carbon fiber tows with resin under compression, enabling the production of complex geometries while reducing material waste.

Finally, the chapter examines the advantages and limitations of composites compared to conventional engineering materials such as metals, addressing issues of cost, recyclability, and environmental impact. These considerations are particularly relevant to the sustainability focus of this thesis.

2.2 Definition

A composite material is formed by combining two or more distinct materials to create a new one with enhanced properties and performance compared to its individual components. These constituent materials remain separate and identifiable at the macroscopic scale, resulting in a heterogeneous structure with a clear interface between phases. Mixtures or solid solutions such as alloys or homogeneous plastics, where materials are combined at the microscopic level, are therefore not considered composites. Typically, a discontinuous phase (known as the reinforcement) is embedded within a continuous phase, referred to as the matrix. In the case of Forged Carbon Fiber, which is the focus of this study, the reinforcement consists of short, randomly oriented carbon fibers dispersed within a continuous polymer matrix.

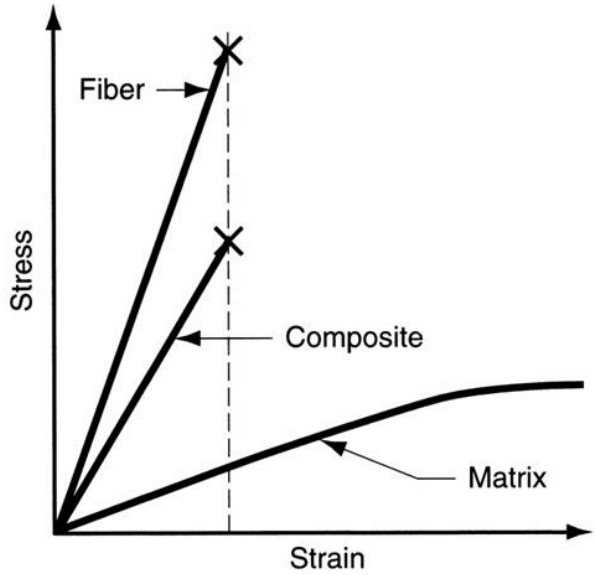

Figure 6 Stress-Strain diagram for composite material in relation to matrix and fiber [20].

Composite materials combine the most advantageous properties of their constituent components; as seen in Figure 6, often resulting in materials that exhibit superior or entirely new characteristics, while maintaining a significantly lower weight compared to traditional materials. This lightweight nature is one of the main reasons

behind the growing adoption of composite materials, such as Carbon Fiber and Carbon Fiber Reinforced Polymers (CFRP), in both the aerospace and automotive industries over recent decades. Compared to conventional metallic alloys like aluminum and steel, these composites offer remarkable benefits, including higher specific strength, improved fatigue and corrosion resistance, and excellent thermal insulation, illustrated in Figure 7. Additionally, their manufacturing versatility allows for the creation of complex and detailed geometries that are difficult to achieve with metals.

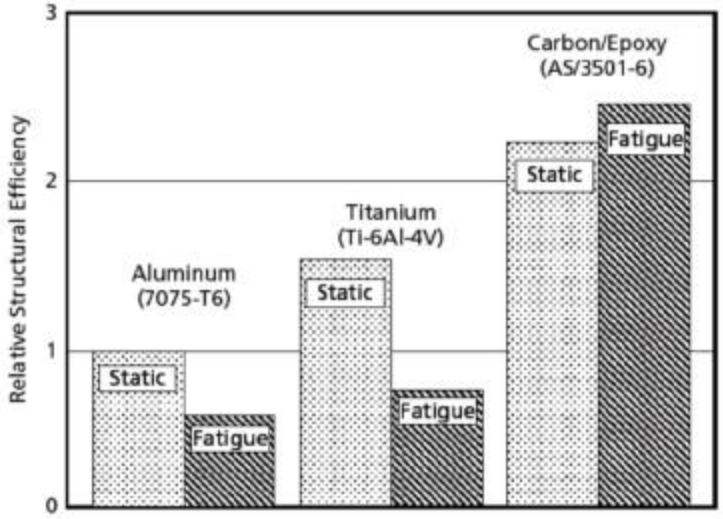

Figure 7 Relative structural efficiency between carbon epoxy composites, Aluminum and Titanium [21].

Weight reduction and damage tolerance are critical requirements in the aerospace industry, where aerodynamic efficiency also demands highly detailed and precise designs. These factors have made aerospace a pioneering field in the development and adoption of composite materials, driving continuous innovation and expansion of their applications.

Composite materials are generally classified into three main categories:

1. Fibrous composites, consisting of fibers embedded within a matrix material.
2. Laminated composites, made up of multiple bonded layers that may have different orientations or material types.
3. Particulate composites, which incorporate dispersed particles within a continuous matrix.

These classifications can also be combined in certain structures, depending on the design requirements. In the context of the present work, the focus is placed on

discontinuous fibrous composites, such as forged carbon fiber, which differ from traditional laminated composites in structure and manufacturing approach; represented in Figure 8, but offer unique advantages in terms of formability and production efficiency.

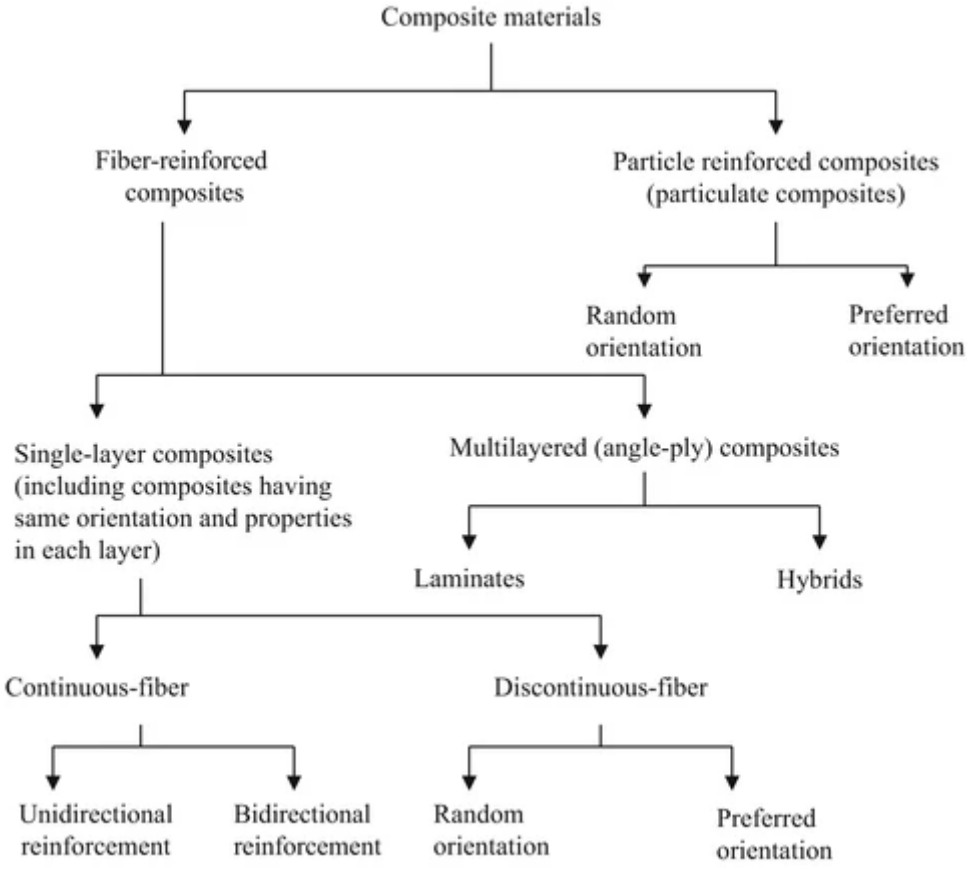

Figure 8 Classification of composites [22].

2.3 Fibrous Composite Materials

2.3.1 Fibers

A fiber is characterized by its high length-to-diameter ratio and extremely small, often crystal-scale diameter. One of the defining properties of fibers is that they exhibit significantly greater strength when used in elongated form compared to the bulk material. For example, while conventional glass is brittle and fractures at around 20MPa, glass fibers can reach tensile strengths of 1000–3500MPa. This improvement arises from the fiber's refined structure and reduced internal defects, which enhance

strength and stiffness. Thus, fiber geometry and microstructural integrity play a crucial role in determining the final performance of fiber-reinforced composites [22].

Among the various fibers available, carbon fiber is the most widely used in modern composite applications due to its exceptional mechanical performance, combining high tensile strength (around 5000MPa) and stiffness (approximately 250GPa) with low density. Carbon fibers are typically produced from precursors such as rayon, PAN (polyacrylonitrile), or petroleum-based pitch, with PAN being the most common due to its superior balance of cost, processability, and mechanical properties. Rayon-based production methods, though historically significant, have largely been phased out due to lower yield and higher cost.

Pitch-based fibers, on the other hand, are often employed when very high or ultra-high modulus fibers are required, as they can be carbonized at about 1700°C in an inert atmosphere—or at even higher temperatures for graphitization, these processes are represented in Figure 9. Owing to their small diameter, carbon fibers can be woven into fabrics or used as tows, which are untwisted bundles containing thousands of filaments (typically 1K, 3K, 6K, 12K, or 24K). To enhance bonding with the matrix material, carbon fibers generally undergo surface treatments that improve interfacial adhesion [23].

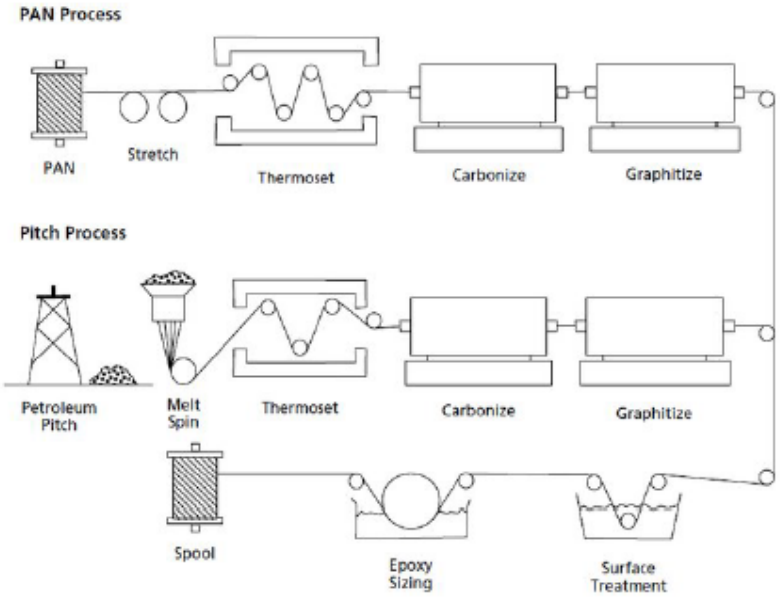

Figure 9 Fiber manufacturing using PAN and Pitch processes [23].

In the context of forged carbon fiber, instead of using continuous or woven fiber tows, these carbon fibers are chopped into short lengths and randomly distributed within a resin matrix. This approach eliminates the need for weaving and lamination, while still benefiting from the intrinsic strength of carbon fibers, though with reduced anisotropy and lower directional stiffness compared to continuous-fiber composites.

2.3.2 Matrices

The matrix is the medium in which the fibers are embedded and bonded, maintaining their position and orientation while enabling stress transfer between them. It also provides protection against heat, moisture, and chemical exposure. An effective matrix should exhibit good strain-to-failure, low curing temperature, long out-time stability, and minimal toxicity. Matrices can be made from polymers, metals, ceramics, or carbon, depending on the desired properties and application.

Polymers are the most common type of matrix and can exist in several structural forms: linear, branched, and cross-linked as shown in Figure 10. Linear polymers consist of single molecular chains, branched polymers include side-chain extensions, and cross-linked polymers form three-dimensional networks. Their strength generally increases from linear to cross-linked structures.

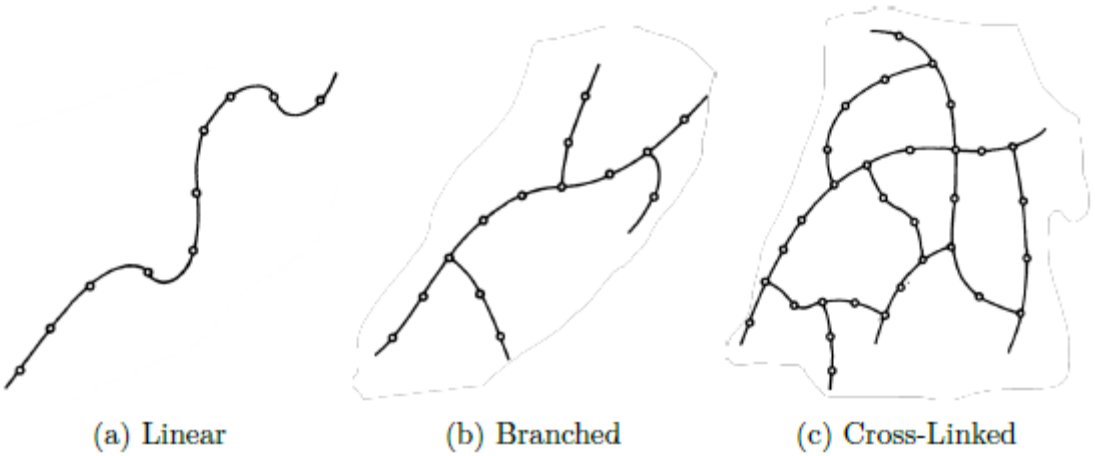

Figure 10 Polymer structures [24].

Polymers are typically classified into three main categories:

- Rubbers, which are lightly cross-linked polymers that behave as semicrystalline solids at low temperatures and as elastic materials above room temperature.
- Thermoplastics, which are linear or branched polymers that soften when heated and harden upon cooling. They can be reshaped multiple times and include materials such as nylon, polyethylene, and polysulfone.
- Thermosets, which undergo irreversible chemical cross-linking during curing, resulting in rigid, three-dimensional structures that cannot be remelted. Examples include epoxies, phenolics, and polyimides.

Unlike thermosets, thermoplastics can be reprocessed by reheating to high temperatures, allowing for reshaping and recycling. In addition to polymer matrices, metal matrices—such as aluminum, titanium, and nickel-chromium alloys—can be formed by diffusion bonding or vacuum infiltration around fibers, offering superior thermal and mechanical properties for specialized applications [24].

2.3.2.1 Epoxy Resins

Epoxy resins are a class of thermosetting polymers, which means that after a reaction occurs, the material solidifies permanently. Epoxy resins provide a matrix for the fibers to set in and maintain proper position and orientation. They protect against stresses by distributing loads across multiple fibers and dissipating localized effects. Furthermore, resins offer resistance to heat, chemicals, and moisture. The most common thermoset resins used as matrices are polyesters, epoxies, vinyl esters, bismaleimides, polyimides, and phenolics, as seen in Table 1 [25].

Thermoset resins mainly consist of a resin and a matching curing agent, also known as a hardener. When the two are mixed, the composition begins curing after heat is applied, either exothermically or endothermically. During the curing process, as previously discussed in Section 2.2, a series of molecular links are formed, creating a large, solid, and irreversible network. The curing process involves the resin and curing agent reaching a temperature known as the Glass Transition Temperature (Tg). When heated past this temperature, the polymer exhibits a rubbery behavior, and upon cooling back below it, the resin becomes glassy, permanently hard, shrunken, and brittle. Unlike the melting point of conventional materials, exceeding Tg does not

cause structural collapse, though the structure may degrade if heated beyond the Decomposition Temperature (Td), represented in Figure 11.

This curing process usually takes place inside an autoclave, a machine that applies both heat and pressure to help composites achieve their final permanent form. However, depending on the resin system, curing can sometimes also occur at room temperature, especially in formulations designed for out-of-autoclave or ambient curing conditions [21, 23].

Table 1 Characteristics of resin matrices for composites [21].

Material	Description
Polyesters	Used broadly in commercial applications. Inexpensive and easy to process. Utilized in both continuous and discontinuous composites
Vinyl Esters	Similar to polyesters, but stronger and more resistant against moisture.
Epoxies	Used for high performing matrices, mainly for continuous fiber composites. Better performance for high temperatures (120°C-135°C) than polyesters and vinyl esters.
Bismaleimides	Utilized in high temperature (135°C-175°C) resin matrices, with similar processing to epoxies. Requires post-cure at elevated temperatures.
Polyimides	Curing at extremely high temperatures (290°C-315°C), making it very difficult to process.
Phenolics	For high temperature resin solutions, with smoke and fire resistance. Common in aircraft interiors, however it is hard to process.

Epoxy resins are the most widely used thermosets since they have a relatively low molecular weight and exhibit minimal shrinkage during curing. In addition, epoxies can be partially cured and stored in that state—typically in a freezer—for future use, as is common with pre-impregnated composite materials. They possess excellent mechanical properties, along with high resistance to temperature, chemicals, and corrosion. For epoxies, Tg generally ranges between 100°C and 270°C, and the curing agents are often aromatic amines such as 4,4-Methylene-Dianiline-Amine (MDA) and 4,4-Sulfonyldianiline (DDS) [23].

During the curing phase—typically in an autoclave—the resin hardens and defines the final geometry. The properties of epoxy provide composite materials with key advantages, including toughness, rigidity, stiffness, high-temperature performance, and excellent adhesion.

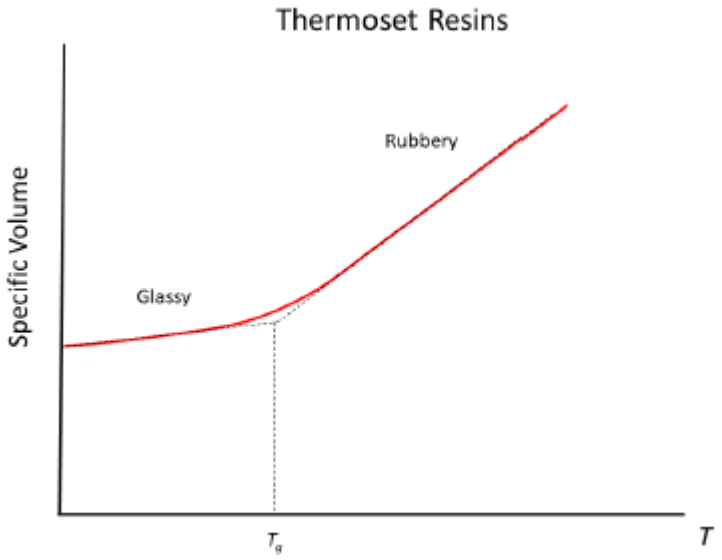

Figure 11 Specific volume variation against temperature and glass transition temperature [26].

2.3.3 Forged Carbon Fibers

Having discussed fibrous composite materials in Section 2.3, forged composite materials can now be introduced as it is one of many methods to produce Fibrous Composite Materials, specifically it is a type of Sheet Molding Compound (SMC). Forged Carbon Fiber is a type of discontinuous fiber-reinforced composite, consisting of short or chopped carbon fibers randomly distributed within a resin matrix. Unlike laminated composites, which are made of continuous woven layers, forged composites use a bulk mixture of carbon fibers and resin, allowing for the formation of complex geometries without the need for manual layering or orientation control.

Figure 12 Forged carbon fiber components [27].

The manufacturing process involves placing the fiber-to-resin mixture into a mold, which is then subjected to heat and pressure—typically in a compression molding press or autoclave—to cure and consolidate the material into its final shape. This process results in a dense and uniform structure where the short fibers are randomly oriented, giving the material isotropic mechanical properties and eliminating the directional weaknesses found in traditional laminated composites.

The properties of forged carbon fiber depend on several factors, including fiber length and distribution, fiber-matrix adhesion, and the molding parameters such as temperature, pressure, and curing time. Compared to laminated composites, forged composites generally have lower tensile strength and stiffness due to the absence of continuous fibers, but they exhibit higher impact resistance, better damage tolerance, and improved formability [28].

Additionally, the ability to fill molds of complex shapes without manual layup significantly reduces manufacturing time and cost, while improving repeatability and scalability. These characteristics make forged carbon fiber suitable for applications requiring lightweight, strong, and geometrically intricate components, such as in automotive, aerospace, and consumer product industries.

In summary, forged carbon fiber combines the advantages of high-performance carbon fibers with the versatility of molding processes, offering an efficient balance between mechanical performance, manufacturability, and design freedom, seen in Figure 12.

2.4 Mechanical Performance of Composite Materials

Conventional materials like alloys are typically homogeneous and isotropic. Homogeneity means that the material exhibits uniform mechanical properties and behavior at every point, while isotropy implies that these properties are independent of orientation, meaning that normal or shear stresses produce the same deformation regardless of direction. In contrast, as seen in Figure 13, composite materials are generally heterogeneous and anisotropic or orthotropic, meaning that their mechanical behavior depends on both position and orientation of the applied stresses. Although this complexity makes composites more challenging to design and model, it also allows for tailored mechanical performance in specific directions, often exceeding that of conventional materials. Combined with their inherent lightweight

nature, these properties explain the extensive use of composites in aerospace, automotive, and high-performance applications.

(a) Sheet of Aluminum alloy. (b) Component of forged carbon fiber.

Figure 13 Comparison between alloy and composite: The composite has multiple distinct materials, while the aluminum alloy appears homogeneous.

In isotropic materials, applying a normal stress causes only extension in the loading direction and contraction in the perpendicular direction, while shear stresses produce only shear deformation. Orthotropic materials behave similarly if the stresses are aligned with their principal directions, though the magnitudes of the responses differ. However, in anisotropic materials, normal stresses can generate both normal and shear deformations, and shear stresses can produce both shear and normal deformations, these differences are illustrated in Figure 13. This coupled mechanical behavior is an essential consideration in the design and analysis of composite structures [23].

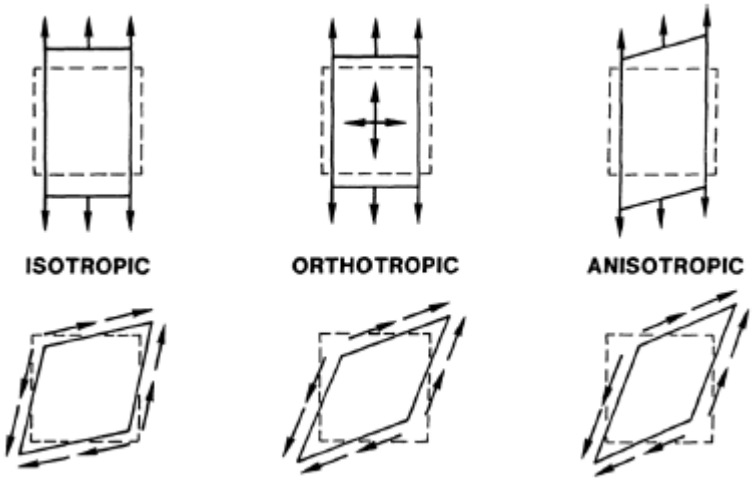

Figure 14 Mechanical behavior of various materials during stress application [24].

In the case of forged carbon fiber composites, the random orientation of short fibers within the resin matrix leads to a structure that behaves quasi-isotropically by nature. Unlike laminated composites—where fibers are deliberately oriented in specific directions to manage stresses—short fiber composites achieve a more uniform response under multi-directional loading due to the random distribution of fibers. This means that the mechanical properties are similar in all directions, reducing the need for complex layer stacking or orientation control. In any case, the focus of this metamaterial is to achieve acoustic characteristics, hence rendering the randomness to become an advantage due to its distortion properties.

While this random orientation may slightly reduce stiffness and strength compared to continuous-fiber laminates, it offers significant advantages in terms of damage tolerance, manufacturability, and isotropic-like mechanical performance. The distributed stress response in forged composites helps prevent localized failure, as the applied load is spread across many randomly oriented fibers and through the resin matrix, seen in Figure 15. This results in improved impact resistance, fatigue behavior, and crack propagation resistance. [24]

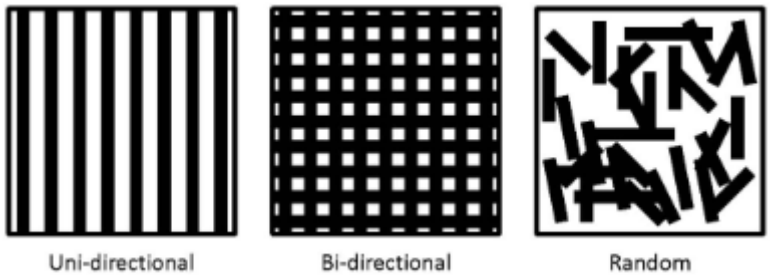

Figure 15 Difference in fiber orientation [29].

Overall, the quasi-isotropic behavior of forged carbon fiber provides a mechanical response that is more uniform and predictable across different loading directions, while maintaining many of the benefits of composite materials such as high stiffness-to-weight ratio, corrosion resistance, and design flexibility. This makes forged carbon fiber an attractive solution for applications requiring a balance between mechanical performance, weight reduction, and complex geometry manufacturability.

2.5 Compressing Process

The compression molding process represents one of the most efficient and versatile methods for producing composite components, especially when short or discontinuous fibers are employed. In this process, the final geometry of the part is achieved by placing the reinforcing material and the polymeric matrix inside a mold cavity, followed by the simultaneous application of pressure and temperature. This technique ensures consolidation, proper resin impregnation, and the elimination of voids, leading to a compact and structurally sound component.

In the case of FCF, the process slightly differs from traditional compression molding of prepreg materials. Instead of using pre-impregnated sheets, the reinforcement and matrix are introduced into the mold separately. Typically, short or chopped carbon fiber tows are first placed into the mold cavity, either randomly distributed or strategically oriented in regions expected to bear higher stresses. Once the fibers are evenly spread, a liquid thermosetting resin—commonly an epoxy—is poured or distributed across the mold surface, allowing it to infiltrate the fibrous network, this process can be seen from Figure 16 to Figure 18.

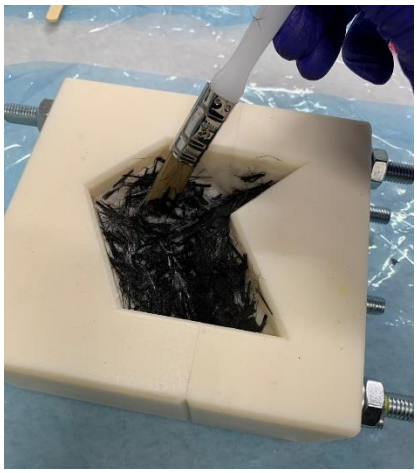

Figure 16 Impregnating short carbon fiber with resin in a mold.

To ensure proper impregnation and eliminate entrapped air, the mold is then closed and subjected to compression using a press or a vice. The applied pressure forces the resin to flow through the fiber network, filling voids and promoting intimate contact between fibers and matrix. This step is crucial, as it determines the fiber volume fraction, void content, and final surface quality of the component. During this stage, temperature may also be applied, depending on the resin system used. Some epoxy resins are capable of curing at room temperature, while others require elevated

temperatures to initiate or accelerate cross-linking reactions. The selected temperature and pressure cycle must therefore be carefully optimized to balance resin flow, curing rate, and fiber movement within the cavity. In our case a room temperature curing resin was chosen.

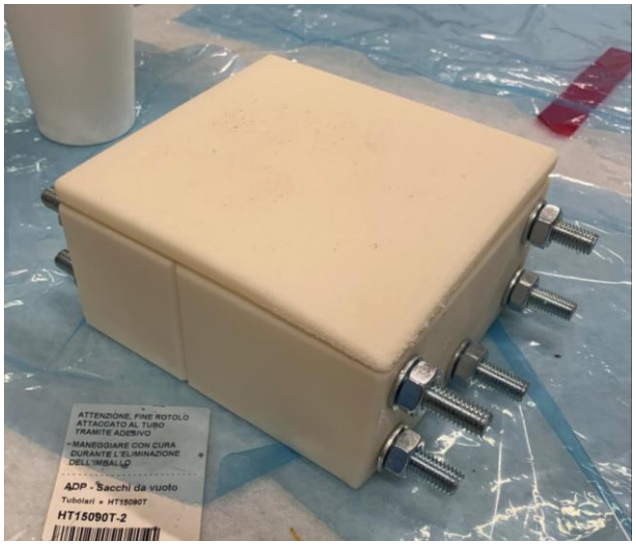

Figure 17 Closed mold compressing the fiber.

The curing process represents a thermosetting reaction, during which the liquid resin transitions into a rigid, cross-linked solid. This phase transformation provides the composite with its final mechanical strength and dimensional stability. When the resin reaches its Tg, the material begins to exhibit rubbery behavior, but as curing continues and the temperature stabilizes, the structure hardens permanently. In some cases, additional post-curing may be performed at a controlled temperature to ensure full polymerization and improve thermal and mechanical performance.

After the curing cycle is complete, the mold is opened and the part is carefully removed. To avoid surface damage or deformation, mold release agents are typically applied prior to molding. Once demolded, the component is allowed to cool naturally to room temperature. Any excess resin or flashing along the edges is then removed through trimming or light machining operations. Depending on the surface requirements, post-processing such as sanding, coating, or polishing may follow.

Figure 18 Open mold that requires post processing.

The compression molding process offers numerous advantages compared to traditional lamination techniques or machined metal counterparts. It allows the rapid formation of complex geometries with minimal manual handling and a significant reduction in production time. Moreover, the method is highly repeatable, when using a metal mold, as the mold precisely defines the geometry and surface finish of the final part. Another major advantage is the ability to use recycled or chopped carbon fibers, which significantly reduces raw material costs and aligns with sustainability objectives by reintroducing carbon fiber waste into a functional product cycle [30].

However, the process also presents certain challenges. The random orientation of fibers within the mold can lead to some anisotropic mechanical properties that are difficult to predict with precision, also every product will be completely different than the other. Achieving uniform fiber distribution is critical, as local concentrations or resin-rich areas may result in weak zones or inconsistent stiffness. Additionally, precise control of temperature, pressure, and curing time is essential to prevent defects such as voids or incomplete curing [30].

In conclusion, compression molding of FCF provides a promising alternative to conventional laminated composites and metallic tooling, particularly in applications that require lightweight structures, rapid production, and lower manufacturing costs. Its adaptability to recycled fiber feedstock and reduced energy consumption make it an increasingly attractive method for both research and industrial applications, especially within sectors emphasizing sustainability and efficient prototyping.

Chapter 3

Design and Manufacturing

3.1 Introduction

Following the theoretical background presented in the previous chapters on additive manufacturing technologies and composite materials, this chapter focuses on the practical implementation phase of the research. The main objective of this work is to manufacture a complex-shaped acoustic metamaterial in carbon fiber. The use of the FCF technique was specifically chosen due to the unconventional and intricate geometry of the part, which makes traditional composite manufacturing methods less suitable.

The design of the mold represents a crucial step in this process, as it directly influences the dimensional accuracy, surface quality, and mechanical integrity of the final composite piece. To address both cost and accessibility considerations, the decision was made to employ a 3D-printed mold, primarily to reduce manufacturing costs and to evaluate the general viability of using 3D-printed molds in FCF applications. This approach enables rapid prototyping, flexibility in geometric design, and the potential for low-cost experimentation compared to conventional metal tooling.

In this chapter, the complete design workflow is described — starting from the conceptual design of the mold and the choice of printing materials, to the modeling of the desired part and its adaptation to the mold cavity. The part geometry, developed in a previous project by one of the research supervisors, is briefly introduced and referenced here as the foundation of the experimental study.

Finally, the chapter concludes with the description of the experimental procedure used to manufacture the FCF specimen. This includes the preparation of the materials, the molding and compression process, and the first observations related to demolding and surface quality. These steps form the foundation for the following chapter, where the performance of the mold and the resulting composite material will be analyzed and discussed in terms of reusability, mechanical properties, and environmental impact.

3.2 Tools

3.2.1 SolidWorks

SolidWorks is a CAD and Computer-Aided Engineering (CAE) software developed by Dassault Systèmes. It was among the first design programs created for Microsoft Windows, known for its user-friendly interface and relatively low cost. Today, it stands as one of the most widely used and recognized design tools across industries, educational institutions, and among individual users.

Renowned as a solid modeler, SolidWorks allows the creation of mechanical drawings and three-dimensional models composed of one or more parts, which can be either solid or hollow. A key feature that contributes to its status as an industry standard is its parametric design capability—a method that defines models through dimensional and geometric constraints controlling their size, shape, orientation, and position. In SolidWorks, the designer can develop a geometry as a single part or as an assembly of multiple components [31].

Beyond modeling, the software also enables various types of simulations and analyses, such as structural, thermal, and fluid dynamic evaluations. Users can also conduct Finite Element Analysis (FEA) to assess the performance and behavior of their designs under different conditions.

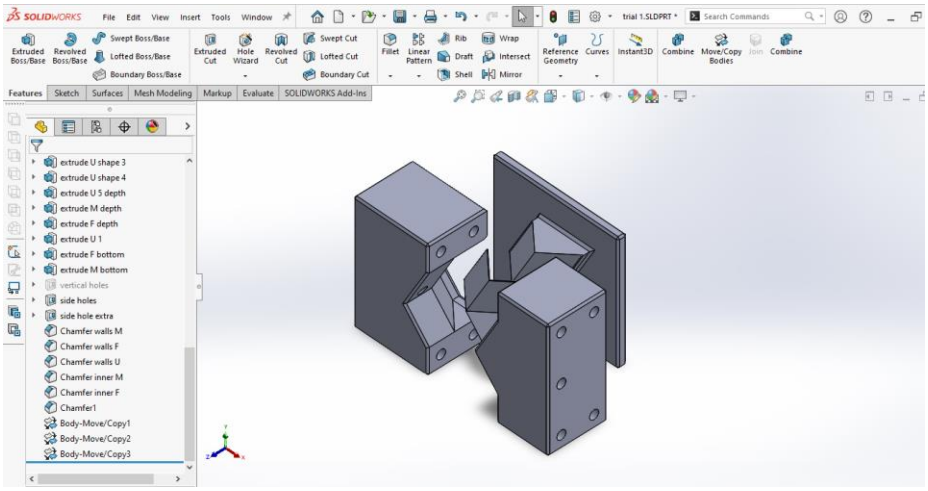

Figure 19 SolidWorks interface.

The mold parts geometries that were used during this learning activities; seen in Figure 19, were designed using this CAD software and then exported into STL file format; shown in Figure 20, which is cutting the geometry into layers for numerical control and recognized by the control software of the 3D printer [31].

The .STLd file format was developed alongside the Stereolithography (SLA) manufacturing process, which explains the shared naming. Also known as Standard Tessellation Language, it remains the primary file format used in additive manufacturing. Once a design is completed in SolidWorks or any similar CAD software, the continuous geometry is converted into a structured file containing a header, a mesh of triangles, or a matrix of X, Y, and Z coordinates with normal vectors defining each triangle's orientation. The smaller the triangles, the higher the fidelity and accuracy of the resulting model [7].

Internal surfaces are defined using the right-hand rule and the rule that vectors and edges cannot intersect at the same point. During slicing, additional edges are introduced, contributing to the discretization error characteristic of Finite Element Methods, where a smooth surface is approximated by a stepped contour. This apparent inaccuracy can be minimized by incorporating small-radius features relative to the geometry's dimensions. Furthermore, the model's height along the Z-axis should be designed so that its total thickness corresponds to an integer multiple of the individual layer thickness used in the printing process [32].

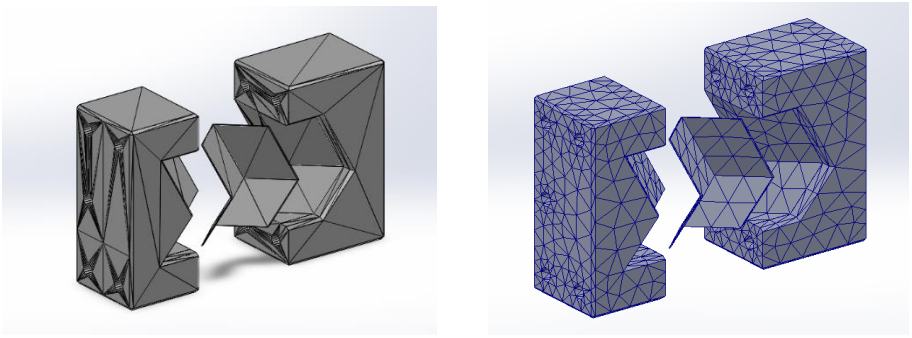

Figure 20 STL model (left) vs graded mesh (right).

3.2.2 Stratasys Fortus 250mc

Stratasys Fortus 250mc is a printer by Stratasys; shown in Figure 21, utilizing FDM additive manufacturing technology. The printer has an enclosed printing chamber, with controlled environment and filament temperature, for optimum results, thus reducing potential risk of deformation.

Figure 21 Stratasys Fortus 250mc printer [33].

The geometry is produced using two continuous spools of thermoplastic filament that are fed into the printer's extrusion head. The print head heats the material until it reaches a molten state and then deposits it layer by layer to form the desired geometry. The material is extruded following a predefined printing pattern onto a horizontal build platform, where it cools and solidifies to create a surface upon which subsequent layers are added. This process is repeated iteratively along the vertical (Z) axis until the complete three-dimensional model is formed. The printer's total build volume is (X × Y × Z): (254mm × 254mm × 305mm). Typically, during the initial printing stages, additional material is required to form support structures that stabilize the geometry and prevent deformation, shifting, or buckling throughout the printing process. These supports are often made using different materials or printing patterns to facilitate easier removal during post-processing and to minimize material usage.

The materials utilized in the printing process are ABSplus P430 (Acrylonitrile Butadiene Styrene) for the primary filament and SR-30 for the support structure. Both materials are supplied in proprietary cartridges developed by Stratasys, meaning their

specific compositions and characteristics are unique to the company's printer range. The layer thickness used in printing varies between 0.178 mm and 0.330 mm. While the main filament is available in a range of colors, the support material is exclusively provided in white. The volume of available filament per cartridge for both materials is 923cc. For this thesis, we mostly utilized the main filament; since the geometry did not require any support material to be built except for the raft, as we needed the mechanical and thermal properties of ABSplus P430. In this specific printer model, the printing plate is also regarded as a consumable component. After each print, a thin layer of material residue remains on the surface, rendering it unsuitable for reuse. According to the manufacturer, the build platform is designed for single-use only, as reusing it may lead to calibration inaccuracies and compromised print quality [33].

Table 2 Mechanical and thermal properties of ABS P430 [34].

MECHANICAL PROPERTIES[1]	TEST METHOD	ENGLISH	METRIC
Tensile Strength (Type 1, 0.125", 0.2"/min)	ASTM D638	3,200 psi	22 MPa
Tensile Modulus (Type 1, 0.125", 0.2"/min)	ASTM D638	236,000 psi	1,627 MPa
Tensile Elongation (Type 1, 0.125", 0.2"/min)	ASTM D638	6%	6%
Flexural Delamination	ASTM D790	2,000 psi	14 MPa
Flexural Strength (Method 1, 0.05"/min)	ASTM D790	6,000 psi	41 MPa
Flexural Modulus (Method 1, 0.05"/min)	ASTM D790	266,000 psi	1,834 MPa
IZOD Impact, notched (Method A, 23°C)	ASTM D256	2.0 ft-lb/in	106 J/m

THERMAL PROPERTIES[2]	TEST METHOD	ENGLISH	METRIC
Heat Deflection (HDT) @ 66 psi	ASTM D648	195°F	90°C
Heat Deflection (HDT) @ 264 psi	ASTM D648	169°F	76°C
Glass Transition Temperature (Tg)	DMA (SSYS)	219°F	104°C
Melt Point	---------	Not Applicable[3]	Not Applicable[3]
Coefficient of Thermal Expansion	ASTM E831	5.60 E-05 in/in°F	---------

From the listed properties in Table 2, several key characteristics make ABSplus P430 a suitable material for the 3D-printed mold. Its moderate tensile and flexural strengths (22MPa and 41MPa, respectively) ensure that the mold can withstand the compression forces applied during the Forged Carbon Fiber process without significant deformation. The high flexural modulus (1.84GPa) provides the necessary stiffness to maintain dimensional accuracy, while the impact resistance of 106 J/m helps absorb localized stresses during clamping and demolding. Thermally, the heat deflection temperatures of 76–90°C and glass transition temperature of 104°C guarantee that the mold remains stable under the exothermic curing reaction of the epoxy resin, preventing warping or softening. Together, these properties allow ABSplus P430 to offer a reliable balance of strength, toughness, and thermal stability for repeated use in low-temperature composite forming applications.

The printer connects to the computer network via an Ethernet interface, allowing one or more computers equipped with the Stratasys Fortus software to manage and process print jobs. These software include the programs Insight and

Control Center. The Insight software takes an .stl file as input, enabling the user to configure various printing parameters such as the filament type (main or support), material density (low sparse, double dense, or high sparse), filament line width, and support structure type. The support configuration can be set to SMART mode for automatic adjustment based on the geometry or manually selected as square or other predefined shapes, illustrated in Figure 22 (a).

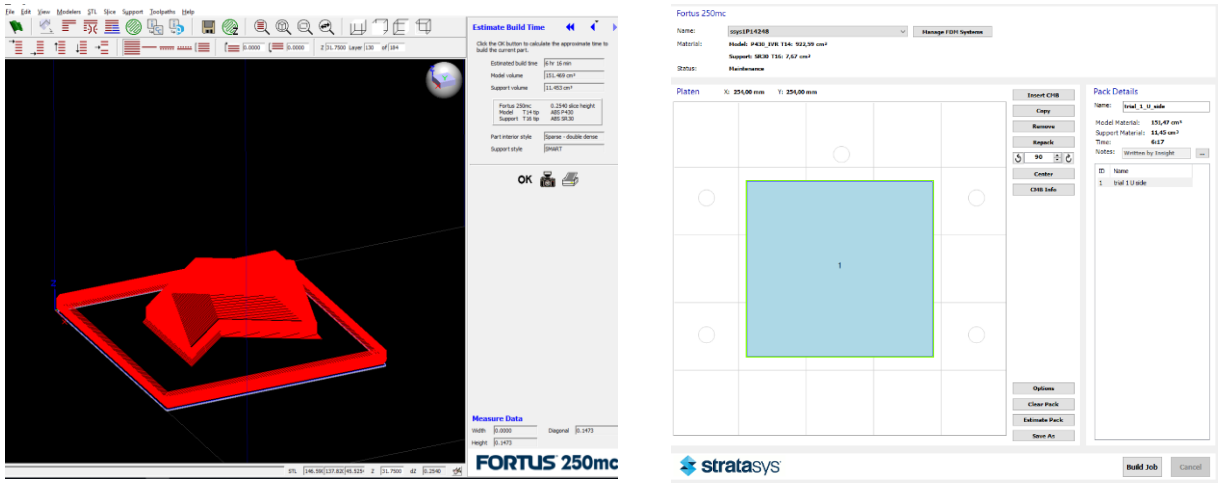

(a) (b)

Figure 22 Workflow of (a) Insight and (b) Control Center.

Once the settings are confirmed, the software generates the nozzle path for all the layers required to complete the print, creating a file that is then managed by the Control Center software, seen in Figure 22 (b). The Control Center takes one or more files produced by Insight and allows the user to arrange their placement on the build platform. It also calculates the amount of filament needed for the print by communicating with the printer to verify the available material in the cartridges. Multiple parts can be printed simultaneously, as the print head forms a common layer surface for each component in the specified order.

The selected printing pattern, material density, and support configuration directly influence both the printing duration and the amount of material consumed. Given the importance of sustainability and minimizing plastic usage, careful consideration should be given to the chosen density settings to balance material efficiency with the required structural strength.

3.3 Design of the Composite Geometry

The starting point of this research was the definition of the composite part to be produced. The geometry of the desired component was originally developed and analyzed in the framework of a previous project by PRIN project DAMA, where its mechanical and structural characteristics were investigated through numerical and experimental methods. According to the research done, the geometry has been conceptualized by the means of vibro-acoustic optimization design and then it was made into a periodic structure for applications in aircraft fuselage panels as a response to the noise and vibrations problem that the aircraft exhibits [35].

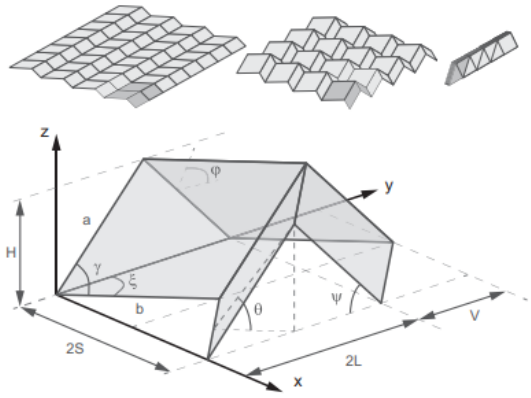

Figure 23 Scheme for the design of Miura-Ori unit cell [36].

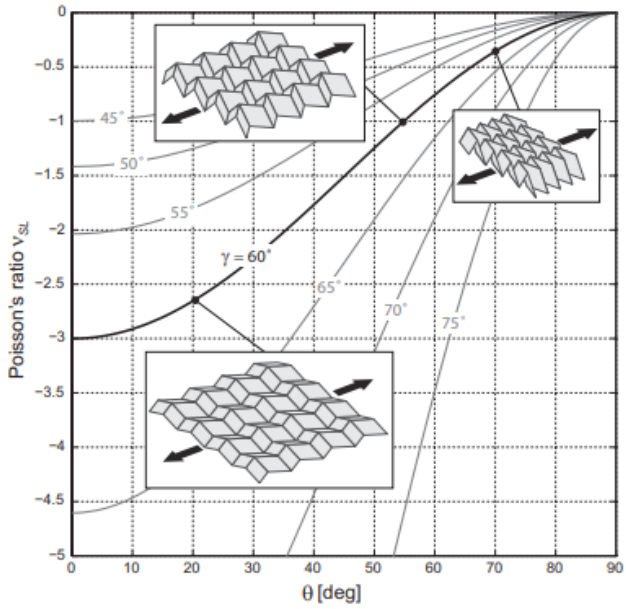

Figure 24 The In-plane expansion coefficient of a Miura-Ori sheet [36].

In the present work, the geometry seen in Figure 23 is adopted as the basis for the manufacturing process, serving as a benchmark for assessing the feasibility of producing such a complex structure using the FCF technique and a 3D-printed mold.

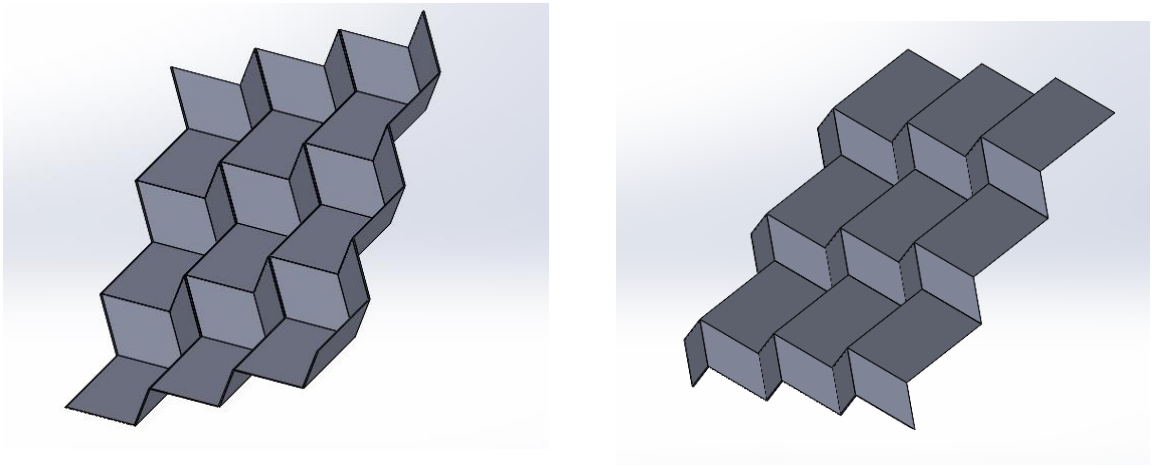

(a) (b)

Figure 25 Final geometry required to manufacture / (a) bottom view / (b) top view.

The component is characterized by a non-conventional metamaterial structure, composed of a repeating unit cell designed to achieve specific stiffness-to-weight and energy transfer mechanism for noise absorption. The geometry involves intricate internal features and undercuts, as seen in Figure 25, which make it particularly challenging to reproduce with traditional composite manufacturing methods such as hand lay-up or resin transfer molding (RTM), specifically the edge quality. These limitations motivated the use of the FCF process, which is more adaptable to complex geometries and allows the carbon fibers to flow and orient freely within the mold cavity under compression.

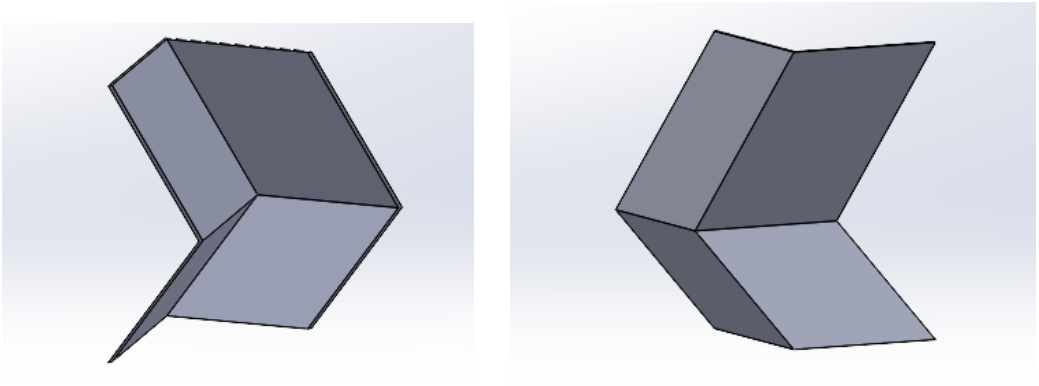

(a) (b)

Figure 26 Single unit cell for experimenting / (a) bottom view / (b) top view.

For the purpose of this study, a single unit cell of the metamaterial was selected as the experimental reference, shown in Figure 26. This smaller-scale model enables the evaluation of the manufacturing parameters, mold performance, and material behavior under compression while minimizing material waste and processing time. The ultimate objective is to scale the process to a four-unit-cell configuration, corresponding to the final target design, illustrated in Figure 27, once the feasibility and reliability of the single-cell fabrication are demonstrated. Successfully achieving the four-unit-cell, configuration would also validate the potential to scale the process further, demonstrating the adaptability of the method to larger and more complex structures.

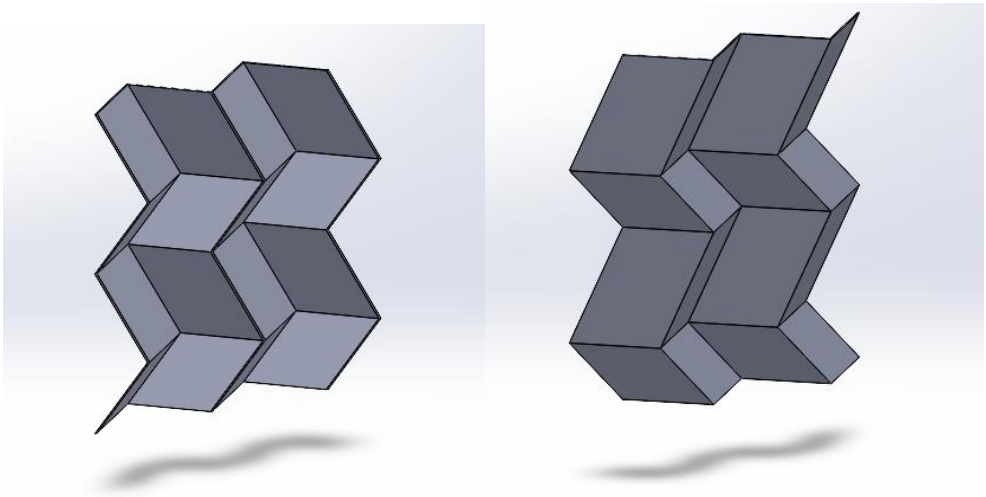

(a) (b)

Figure 27 Four-unit cells required / (a) bottom view / (b) top view.

The 3D geometry of the unit cell was obtained in a digital format and adapted for manufacturing. A minor modification was made to improve printability and mold separation, which was the slight adjustment to wall thickness. The finalized model was then used as the reference geometry for designing the corresponding 3D-printed mold, described in section 3.5.

3.4 Material Selection

The material selection process plays a vital role in the realization of the desired product as it controls the properties of both the mold and the composite. The material selection process was guided by two main objectives: producing a carbon fiber composite part with noise reduction properties and ensuring the mold could be manufactured cost-effectively while maintaining sufficient durability for the compression process. Both the composite and the mold materials were therefore carefully chosen based on mechanical performance, manufacturability, and sustainability considerations.

3.4.1 Composite Material

The primary objective of this work is to manufacture the designed part using carbon fiber. Due to the intricate geometry of the metamaterial such as having straight corners and such a thin thickness (1mm), conventional manufacturing methods like hand lay-up or lamination would pose significant challenges in fiber placement and being able to create 90° angles, also having a very small geometry would pose some issues. For this reason, FCF was selected as the composite manufacturing approach.

3.4.1.1 Carbon Fiber

As discussed previously in Section 2.3.1, carbon fiber stands among the most advanced materials available for lightweight structural applications, particularly in the aerospace and automotive industries. Its exceptional mechanical performance, combined with its low density, makes it ideal for applications where strength-to-weight ratio is critical. Even though the aim of the structure is not mechanical strength, it still needs to hold some mechanical loads as it will be used in an aircraft inside the lining panels as a core of a sandwich.

In this work, FCF technology was chosen as the composite manufacturing approach. Unlike conventional continuous-fiber composites, which rely on carefully oriented plies, FCF utilizes chopped carbon fiber tows dispersed within a thermoset resin matrix. In this study, 6K T300 carbon fibers chopped to a length of approximately

12 mm were employed, seen in Figure 28 and its properties are seen in Table 3. These fibers fall within the category of short to moderately long chopped fibers, providing a compromise between mechanical integrity and geometric adaptability. The random orientation of the short fibers allows the material to conform to intricate shapes while maintaining a relatively isotropic mechanical response.

(a) (b)

Figure 28 CT-12 carbon fiber / (a) virgin / (b) compressed [27].

Table 3 Mechanical and thermal properties of T300 CF [37].

Fiber Properties	Value
Tensile Strength	3530MPa
Tensile Modulus	230GPa
Strain of Failure	1.5%
Density	1.76g/cm3
Filament Diameter	7μm
Coefficient of Thermal Expansion	-0.41×10^{-6} /°C
Specific Heat	0.777J/g·°C
Thermal Conductivity	0.105J/cm ·s·°C
Electric Resistivity	1.7×10^{-3} Ω·cm

As already discussed, one of the key advantages of adopting the Forged Carbon Fiber process lies in its ability to accommodate complex geometries that would otherwise be difficult or impossible to achieve with traditional lay-up techniques. The part investigated in this work, characterized by a metamaterial pattern designed for noise absorption, includes intricate internal features and dimensions that make fiber alignment and layer stacking impractical. The use of short fibers facilitates complete mold filling and uniform reinforcement distribution within these complex cavities.

Beyond manufacturability, the acoustic performance of the composite is another reason for adopting the FCF approach. The random orientation and discontinuous nature of the short fibers promote scattering and diffusion of sound waves, contributing to improved damping and noise reduction capabilities. This microstructural heterogeneity complements the metamaterial geometry, further enhancing the overall noise attenuation effect.

While the use of short, randomly oriented fibers generally results in lower stiffness and tensile strength compared to continuous-fiber laminates, this trade-off is acceptable for the current application. The primary focus of this work is not to maximize mechanical stiffness but to achieve a combination of adequate strength, lightweight construction, and enhanced acoustic damping. In this context, the forged composite still maintains a high level of structural integrity while offering superior formability and energy absorption characteristics.

3.4.1.2 Matrix

The selection of the matrix material was primarily guided by the processing conditions required for compatibility with 3D-printed molds and by the need for a cost-effective, accessible resin system. Since polymer-based molds are sensitive to elevated temperatures, the chosen matrix needed to cure at or near room temperature to avoid thermal deformation or damage to the mold during processing. Therefore, a low-temperature curing epoxy system was considered the most appropriate option [30].

Among the available alternatives, the IN2 epoxy infusion resin paired with the AT30 fast hardener was selected for this work, seen in Figure 29 [27]. This combination provides a convenient processing window suitable for manual handling and compression techniques, with a room-temperature cure that eliminates the need for ovens or autoclaves. Moreover, the IN2 system is widely used in composite

prototyping and small-scale manufacturing due to its excellent mechanical performance, low viscosity (which aids resin flow and wetting of short fibers), and relatively low cost compared to aerospace-grade epoxies.

(a) (b)

Figure 29 (a) IN2 Epoxy Infusion Resin / (b) AT30 Epoxy Fast Hardener [27].

Table 4 Mechanical properties of the cured resin [27].

Resin Properties	Value
Density at Room Temperature	1.08 – 1.12g/cm^3
Hardness at Room Temperature	84 – 88 Shore D
Maximum Tg	82 – 88°C
Water Absorption at Room Temperature (24h)	0.2 – 0.3%
Flexural Strength	107 – 120MPa
Flexural Modulus	2800 – 3200MPa
Compressive Strength	94 – 100MPa
Tensile Strength	74 – 80MPa
Elongation at Break	6.5 – 9.5%
Maximum Strain	5 – 7%
Strain at Break	7 – 12%

3.4.1.3 Mechanical Testing

To assess the mechanical performance of the Forged Carbon Fiber composite, tensile tests should be conducted on specimens produced using the same materials and molding process as the metamaterial unit cell. Although the primary function of the designed component is noise cancellation, its potential application in aerospace structures requires that it also possesses sufficient tensile strength and stiffness to ensure reliability and safety.

The tensile test was carried out according to ASTM D3039/D3039M standards for fiber-reinforced polymer composites. The test consists of applying a uniaxial load to the specimen at a constant crosshead speed until failure occurs, while measuring the applied force and the resulting elongation. The data collected are then used to determine tensile strength, modulus of elasticity, and elongation at break.

Each specimen was molded with the same Forged Carbon Fiber technique used for the actual part, ensuring identical fiber length distribution, resin content, and curing conditions. After curing, the specimens were cut and finished according to standard requirements, ensuring parallel and smooth gripping areas to prevent slippage or premature failure. The test was performed on a universal testing machine equipped with mechanical grips and an extensometer to measure strain accurately in the gauge section.

During testing, the specimen was mounted vertically, and the load was gradually increased until rupture. The load–displacement data were recorded continuously, from which the stress–strain curve could be derived. The tensile modulus was obtained from the initial linear portion of the curve, while the ultimate tensile strength and elongation at break were extracted from the maximum load and total extension, respectively.

This procedure provides baseline data for the material's mechanical integrity, serving as a validation that even though the Forged Carbon Fiber composite is designed primarily for its acoustic properties, it retains adequate structural performance for potential aerospace-related applications.

3.4.2 Mold

The mold was designed to be 3D printed, as additive manufacturing offers a fast, cost-effective, and highly flexible solution for producing custom tooling with complex geometries. The main objective was to evaluate the feasibility of using polymer-based molds for compression molding of Forged Carbon Fiber parts, with a focus on balancing dimensional accuracy, thermal stability, and reusability.

For this purpose, ABS was selected as the mold material. Specifically, ABSplus P430, a commercial-grade filament developed by Stratasys, was employed. ABS was chosen due to its favorable combination of mechanical strength, dimensional stability, and moderate thermal resistance, which makes it suitable for low-temperature composite processing such as room-temperature epoxy curing. Compared to other common FDM materials such as PLA or PETG, ABS provides better toughness and heat deflection capability, allowing it to maintain its shape during the compression of the composite material.

In addition to its mechanical and thermal performance, ABS offers a relatively smooth surface finish and can be post-processed easily through sanding or chemical vapor treatment, if required, to improve surface quality. Its wide industrial availability and consistent print behavior also make it a practical and reproducible material choice for experimental tooling applications.

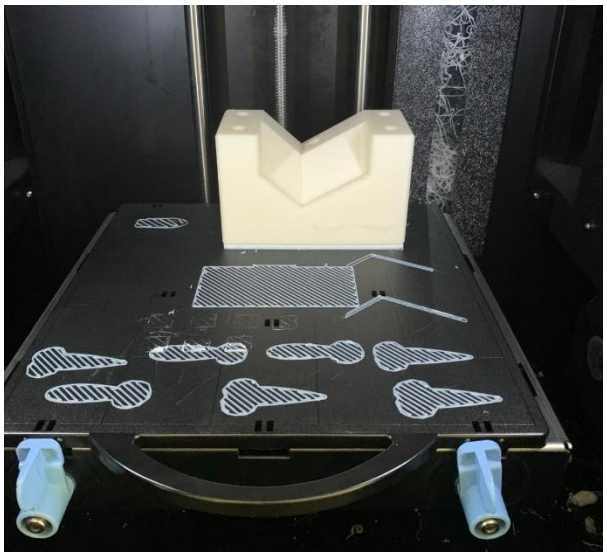

Figure 30 Printed mold part in the Stratasys Fortus 250mc.

The selected material, ABSplus P430, is specifically optimized for Stratasys FDM systems, seen in Figure 30, ensuring controlled extrusion and reliable interlayer adhesion. This guarantees higher dimensional accuracy and reduces the risk of defects such as warping or shrinkage. The choice of this material thus aligns with the broader objective of this work: exploring accessible, low-cost, and reusable mold solutions that can support the sustainable production of composite parts.

3.5 Design of the Mold

3.5.1 Design Objectives and Requirements

The design of the mold plays a crucial role in ensuring the success of the Forged Carbon Fiber manufacturing process. Because the geometry of the metamaterial unit cell is complex and contains intricate internal features, the mold must meet both functional and practical design requirements. It must not only reproduce the desired geometry accurately but also endure the mechanical and thermal conditions of the process while remaining compatible with the limitations of polymer-based 3D printing. The following objectives and requirements guided the design of the mold throughout the development phase.

- Geometric Accuracy: The mold must precisely replicate the geometry of the unit cell to ensure that the final composite part accurately reflects the intended design. Given the metamaterial's complexity, small deviations in the mold could significantly alter the part's acoustic or mechanical behavior. High geometric fidelity was therefore a primary goal, requiring careful consideration of tolerances, surface continuity, and alignment between mold halves.
- Mechanical Integrity: During the compression process, the mold is subjected to mechanical loads as the resin-impregnated fiber mixture is compacted. To prevent deformation or failure, the mold structure must exhibit sufficient rigidity and strength, even when produced using thermoplastic materials like ABS. Reinforcing features such as thicker walls or contour reinforcements were incorporated to increase stiffness while keeping the mold lightweight.

- Ease of Printing: Since the mold was produced using FDM, its design had to accommodate the constraints of additive manufacturing, such as overhang angles, print orientation, and material shrinkage. Avoiding the need for support structures simplified the printing process, reduced material waste, and shortened production time. The design therefore favored self-supporting geometries and straightforward assembly.
- Cost-Effectiveness: One of the main motivations behind using 3D-printed molds was to achieve a low-cost, rapid tooling solution. By optimizing the mold's geometry for minimal material consumption and print time, the overall manufacturing cost was kept low while maintaining acceptable mechanical performance. This makes the approach viable for both experimental research and potential small-scale production.
- Reusability: Another important consideration was the ability to reuse the mold for multiple compression cycles. Although polymer molds are generally less durable than metal ones, the design aimed to extend their lifespan by ensuring uniform stress distribution and avoiding localized failure points. The evaluation of the mold's reusability forms an important part of this study, contributing to the assessment of 3D-printed tooling feasibility in composite manufacturing.

3.5.2 CAD Modeling and Geometric Considerations

The mold was designed using SolidWorks software based on the finalized geometry of the unit cell described in Section 3.3. Several geometric and manufacturing constraints were taken into account to ensure accurate reproduction of the part while maintaining compatibility with FDM technology. Particular attention was given to the definition of parting planes, wall thickness, and alignment features to facilitate both printing and demolding. The resulting CAD model integrates structural reinforcement, assembly precision, and functional simplicity to achieve a robust and manufacturable mold design. The full design workflow was represented from Figure 31 to Figure 40.

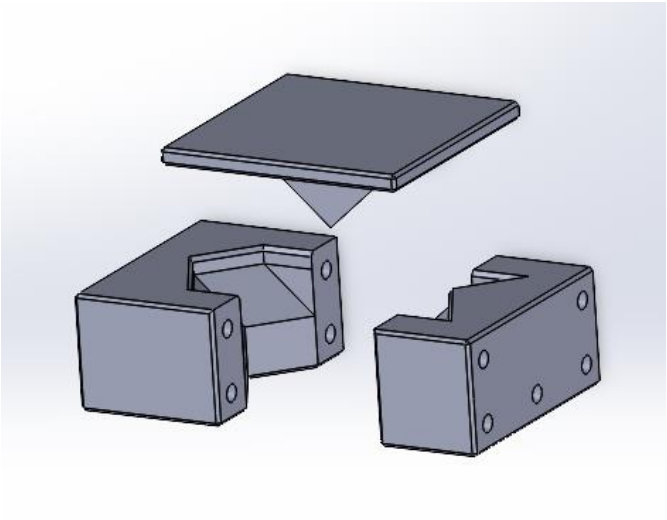

Figure 31 Full design of a one-unit cell mold in exploded view.

The first step for the mold design was to recreate the required geometry in SolidWorks as a single unit-cell; as in mold design the final part serves as the starting point for the entire design, and then the realized geometry was hidden.

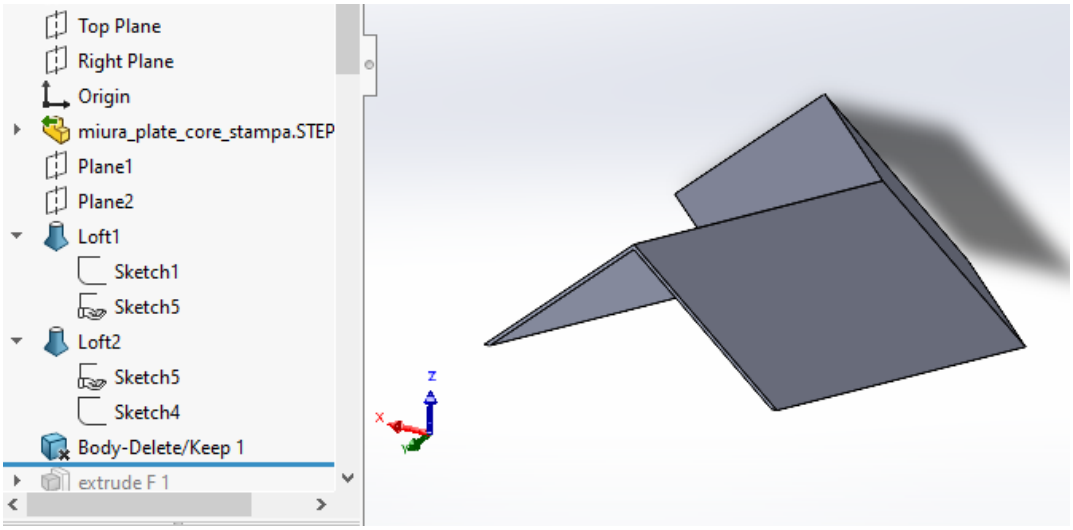

Figure 32 Final geometry design.

Now that the geometry exists, the first step in the mold's design was the walls, starting with the ones along the x-axis. For making the naming process easier, the two molds on the side were named as M and F representing the male and female parts of the mold, as this is a standard technique of mold design that facilitates demolding when the resin is attached to the side parts. It was done by first projecting the shape on the Y-Z plane and extruding it up to the surface and in the other direction 3cm where extruded as a safe measure for heat propagation.

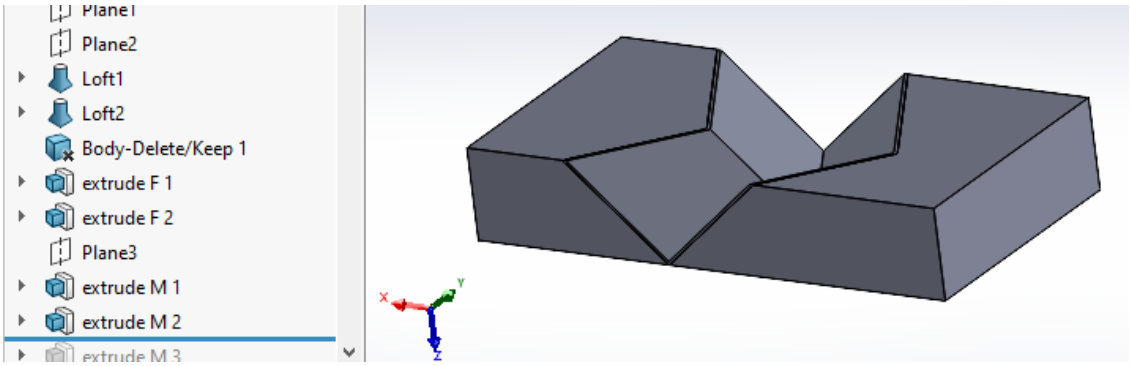

Figure 33 Wall thickness along the X-axis.

Naturally the next step is to create the side walls along the Y axis which were made by the same technique but this time it was an extruded rectangle on the X-Z plane, and it was assured to extrude with the same value of 3cm.The features were merged with their respective sides.

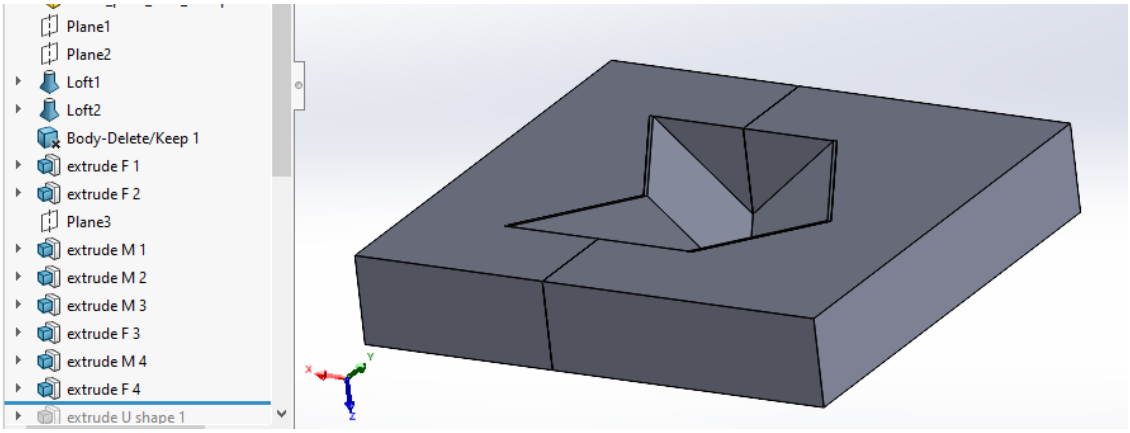

Figure 34 Wall thickness along the Y-axis.

Moving forward, the cover of the mold was created by extruding the negative shape of the part and then adding 1cm of depth to it. The features of the cover were assigned the letter U.

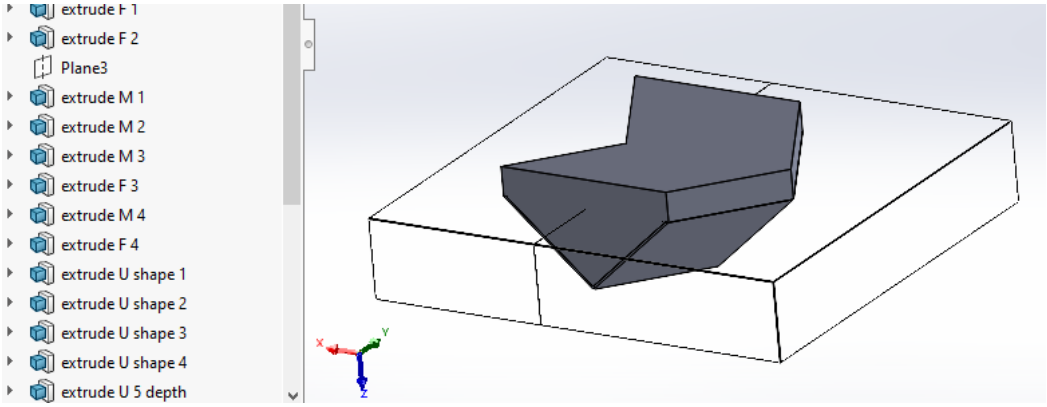

Figure 35 Cover shape and depth.

A tolerance of 0.1mm from all the sides (offset) has been assured between the side pieces and the cover along the Z-axis to make sure the parts don't get locked.

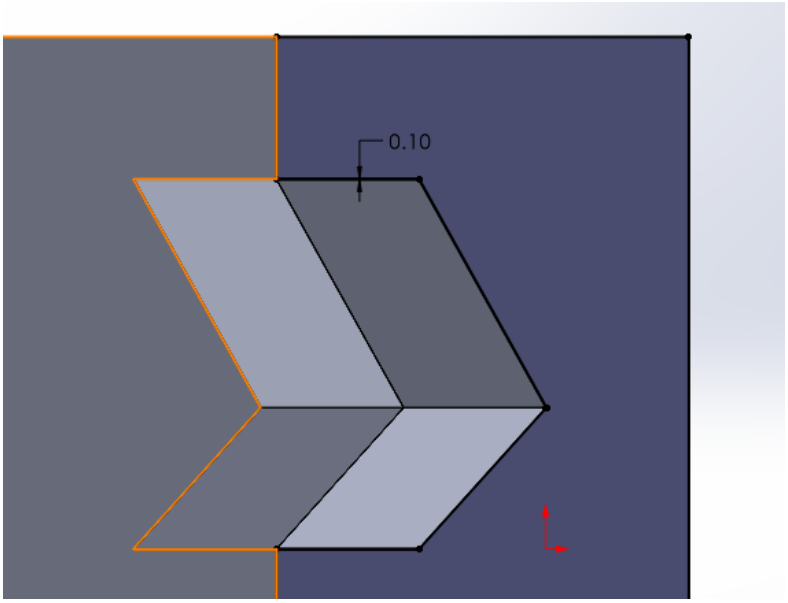

Figure 36 Tolerance between side pieces and cover

Then the cover was realized by adding the full shape of the mold and the bottom depth was extruded as well to finish the basic shape of the mold.

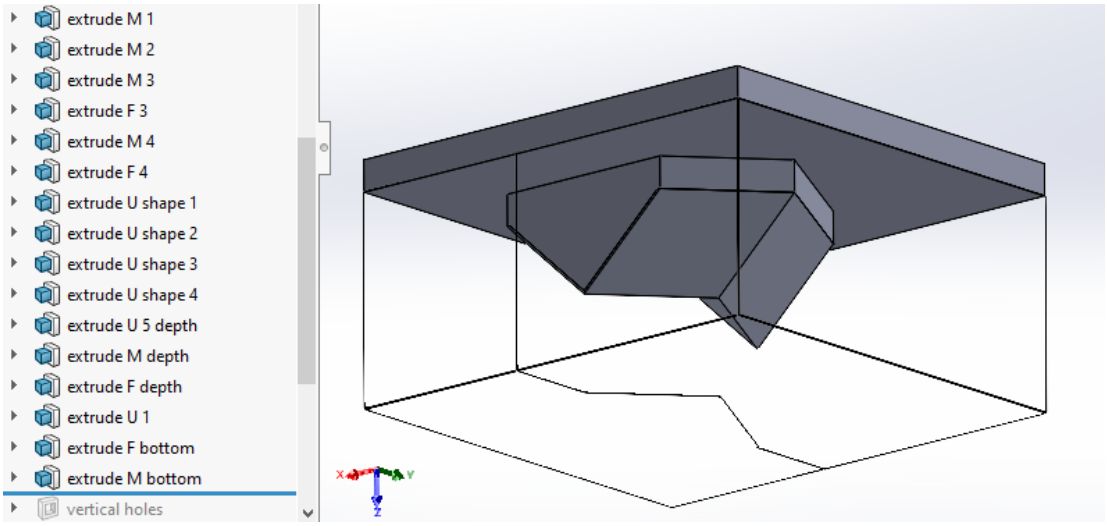

Figure 37 Full cover and M, F depth (bottom view).

The side pieces were then cut with 5 horizontal holes so that the compression would take place with the help of 10M threaded bolts and a tolerance of 0.1mm was guaranteed to avoid lockage due to 3D printing. 4 other vertical holes were made for the compression in the Z-axis but the feature was suppressed because we had access to a vice which would act as a better clamping technique as it has a better stress distribution along the surface.

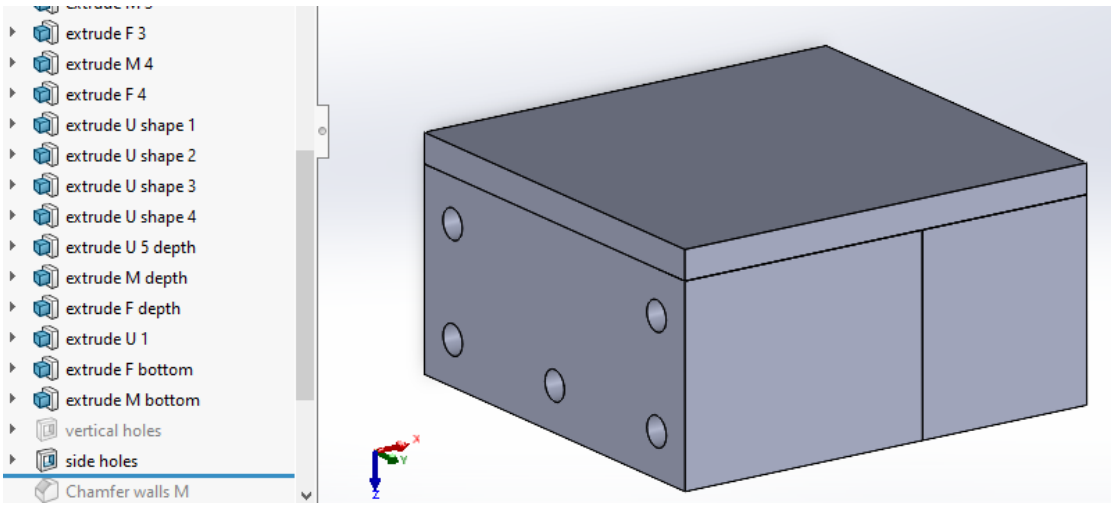

Figure 38 Side holes with suppressed vertical holes.

Afterwards, Chamfers were made along the entire outer surface for two main reasons, the first being that printing any straight edge using the FDM technology could result in expansion of the first layer and affecting the final geometry (also known as Elephant Foot). The second reason is to make a path to guide the tool for the demolding step.

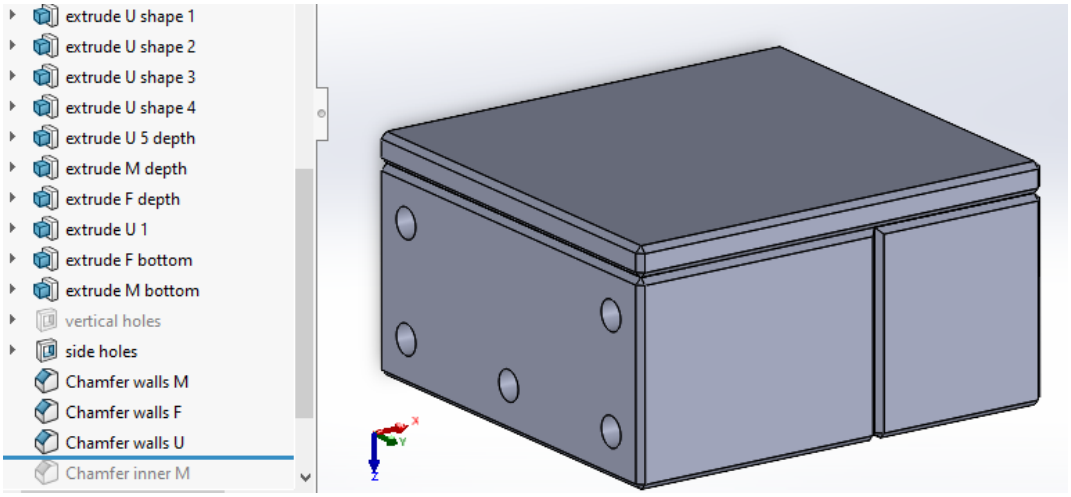

Figure 39 Chamfer on all the outer edges.

Lastly, an inner chamfer was done on the rims of the side molds to create a guide for the cover to go through, similarly, the same chamfer was made on the cover to maintain a tight grip

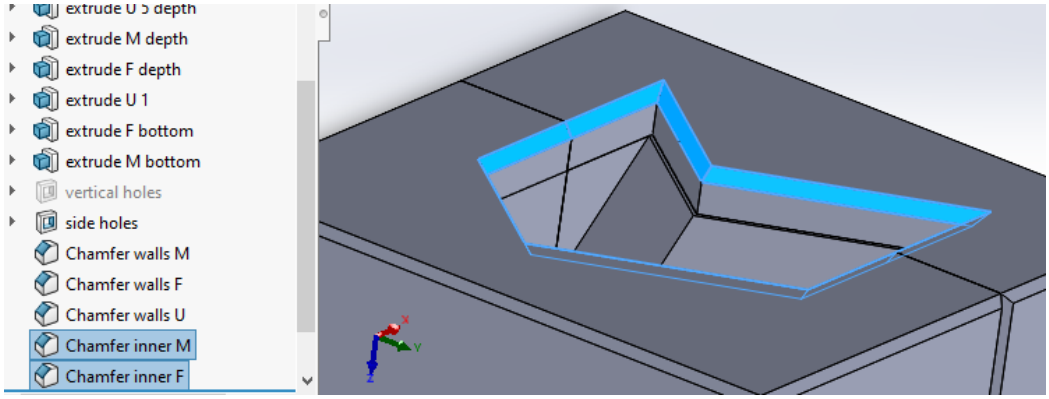

Figure 40 Chamfers on the inner rims.

3.5.3 Printing Parameters and Process Settings

The 3D model of the mold was processed using the proprietary Stratasys Insight software, which converts the CAD geometry into a set of printable toolpaths, a process known as slicing. Slicing involves dividing the digital model into a series of two-dimensional layers and generating the corresponding extrusion paths for each layer, including both the external perimeter (contour) and internal fill pattern (raster).

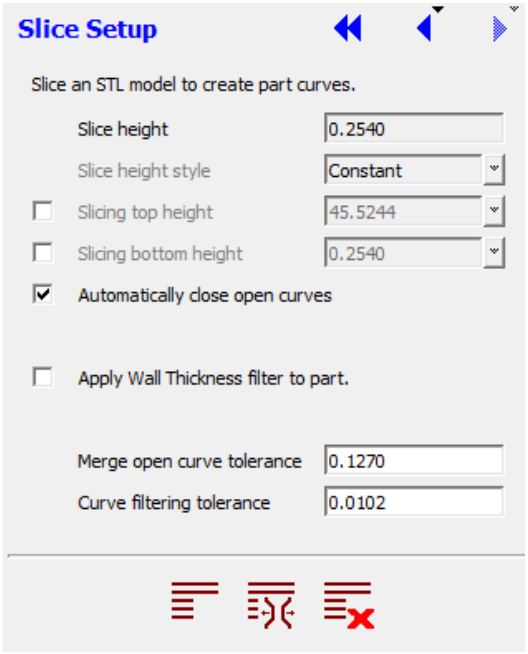

Figure 41 Insight's slicing settings.

A constant slice height of 0.2540mm was used for all parts, as seen in Figure 41, which represents a balanced choice between build accuracy and printing time. This layer thickness ensures adequate detail for the mold's geometry while maintaining sufficient layer bonding strength. All other slicing parameters were kept constant throughout the prints to ensure repeatability and comparability between tests.

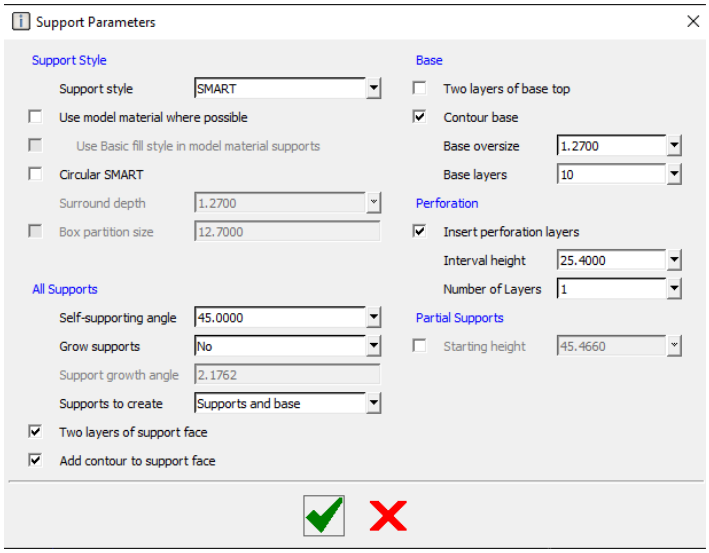

Figure 42 Insight's support settings.

Given the mold geometry was designed with self-supporting angles and partitions, no support structures were generated, as shown in Figure 42. This decision reduced post-processing effort and material waste. However, a raft was added at the base of the mold to improve adhesion to the build platform and minimize warping, which is common with large ABS prints.

Additionally, a perforation layer was introduced between the raft and the printed part. Perforation layers consist of thin layers of model material embedded within the support structure, which facilitate easier detachment after printing and help maintain a clean and undamaged base surface.

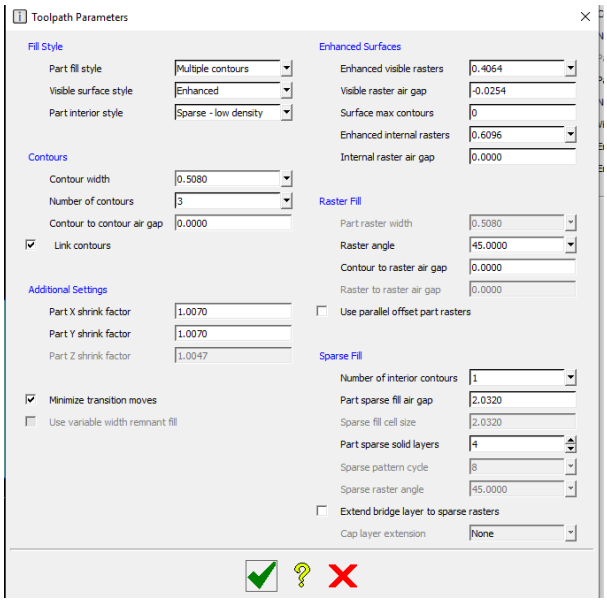

Figure 43 Insight's toolpath settings.

The toolpath parameters were defined to optimize the balance between mechanical strength, dimensional stability, and printing efficiency. The part fill style was set to Multiple Contours, combining solid outer shells with a sparse internal fill, as shown in Figure 43.

- Contour Settings: Three contour lines were used, each with a width of 0.508 mm, and no air gap between consecutive contours. These multiple contours strengthen the outer walls of the mold, providing rigidity and improving surface finish while ensuring tight bonding between adjacent paths. Linking contours ensures continuous tool movement, minimizing weak points along the perimeter.

- Infill Settings: The part interior style was set to Sparse – Low Density, which reduces print time and material consumption while providing adequate internal support to resist deformation during the molding process. The sparse fill was defined with a fill air gap of 2.032 mm, corresponding to a low-density internal structure, and a raster angle of 45° for alternating layers to improve isotropy.

- Enhanced Surfaces: The Enhanced Surface mode was activated to improve visible surface quality and ensure dimensional accuracy on critical mold faces. This setting slightly refines raster overlap and contour definition, leading to smoother surfaces that require minimal post-processing.

3.5.4 Post Processing Treatment

After printing, the mold underwent a series of post-processing steps aimed at ensuring surface quality, dimensional accuracy, and adequate release performance during the Forged Carbon Fiber forming process. Proper post-processing was essential to remove any residual excess material, improve surface smoothness, and prepare the mold surface for composite molding.

The first step involved removing the soluble support material — in this case, limited to the raft layer — using a Stratasys SCA 1200HT cleaning system. The part was immersed in the alkaline solution at 70°C for approximately 4 hours, ensuring complete dissolution of the support without affecting the ABS mold, as seen in Figure 44. This automated cleaning process allowed the part to be uniformly treated and ready for further finishing operations.

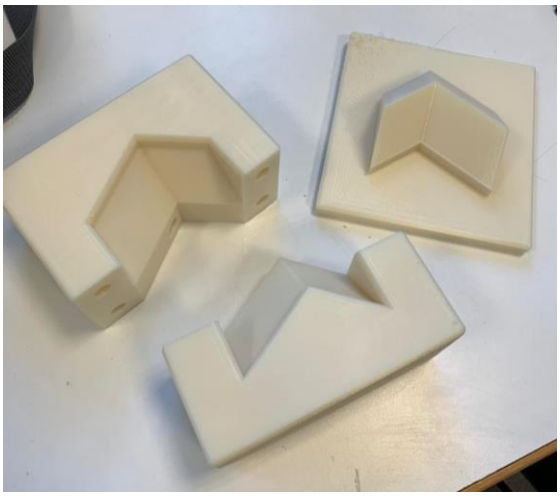

Figure 44 Mold pieces after removing supports.

Following the cleaning stage, the mold surface was manually sanded to eliminate layer lines and minor irregularities left by the FDM process. Sanding was performed progressively using grit papers of 180, 240, 280, 320, and 600, in sequential order. This gradual refinement achieved a smooth, uniform surface that minimized imperfections capable of transferring onto the composite part as seen in Figure 45.

Figure 45 Sanded mold pieces.

Subsequently, a plastic primer coating was applied to improve surface hardness and to seal the porous ABS surface. Three initial layers of primer were applied, with an interval of approximately 10 minutes between coats to allow proper drying. The mold was then lightly sanded again using 600-grit paper to remove excess roughness, followed by the application of two additional primer layers under the same drying conditions. This multilayer coating provided a smooth, sealed surface capable of withstanding contact with epoxy resin during molding.

Finally, to ensure proper demolding and to prevent adhesion between the epoxy matrix and the mold surface, two layers of RW-4 release wax spray were applied, seen in Figure 46. The release agent created a uniform non-stick barrier, facilitating clean part removal and extending the mold's usability for subsequent forming cycles.

Figure 46 Mold pieces after being sprayed with primer and release wax.

3.6 Experimental Procedure

3.6.1 Preparation of the Material

- Material Dosing: The required material quantities were estimated using the manufacturer's guideline, where the cavity volume multiplied by 1.4 gives the total mass of the composite. A 60:40 fiber-to-resin ratio (by weight) was adopted, ensuring good impregnation and structural integrity. The IN2 epoxy infusion resin and AT30 fast hardener were mixed with a 100:30 ratio by weight, as recommended by the supplier [30].

All quantities were measured accurately using a digital balance, and an additional 40% of resin was prepared to compensate for processing losses during mixing and molding.

- Mold Preparation: All mold contact surfaces were checked for cleanliness and dried. Release agent was applied to the mold cavity surfaces as needed to facilitate demolding. The bolts used to clamp the mold were also prepared by applying a thin layer of release wax to their threads and bearing faces to prevent adhesion of any escaped resin and to ease later disassembly.

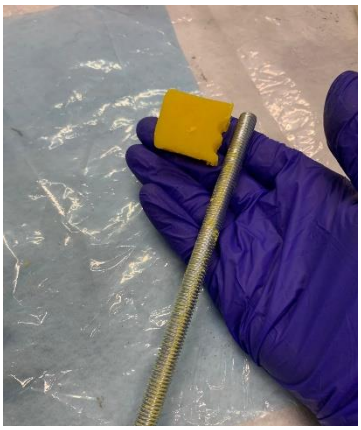

Figure 47 Waxing bolts.

3.6.2 Lay-up and Impregnation

- Initial Resin Layer: A thin, even layer of resin was applied to the mold cavity surface to promote wetting and reduce dry spots when fibers are placed.
- First Half of Fibers: Approximately half of the calculated fiber mass/volume was distributed into the mold cavity (divided by eye), taking care to follow the intended packing pattern for the unit cell. Fibers were distributed to avoid large agglomerations and to fill internal features uniformly.

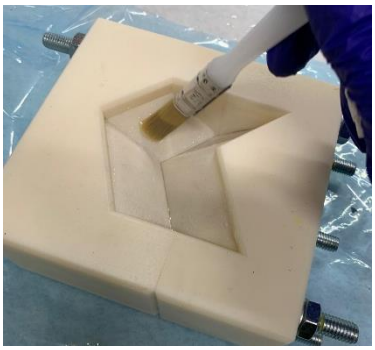

Figure 48 Initial resin layer.

- Impregnation of First Half: The first fiber layer was impregnated using a brush and additional small amounts of resin until visibly saturated. Work was done quickly but carefully within the resin pot life (10-15 mins) to ensure full wetting of the 12mm chopped tows.
- Second Half and Final Impregnation: The remaining fibers were added, distributed evenly, then the whole fiber mass was impregnated thoroughly with the remaining resin, ensuring all voids and cavities were filled and fibers were wetted.

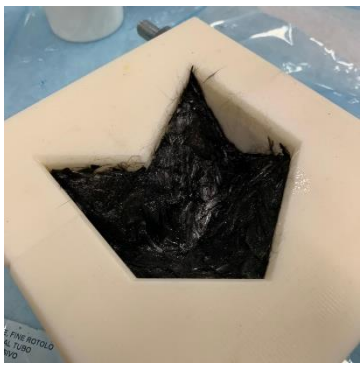

Figure 49 Full impregnated fibers.

3.6.3 Compression and Curing

- Closing and Initial Bleed: The mold halves (male and female) were assembled and bolts inserted. Bolts were hand-tightened or lightly torqued so that the mold closed but not fully tightened; this leaves small gaps allowing excess resin to bleed out during the early compression stage.
- Placing the Assembly in the Vice: The closed mold was placed between the vice jaws sandwiched between two metal plates to distribute the stress evenly. The vice was initially tightened enough to apply a light, even compressive force—firm but not at final clamping strength—again to allow resin to be expelled from the cavity. This stage was held for around 30 minutes to permit resin bleed and initial consolidation. The plastic layer was wrapped around the assembly to collect the spilled resin.

Figure 50 Clamped assembly on the vice.

- Final Clamping and Curing: After the 30-minute bleed period, the vice and bolts were tightened to full clamp force to complete the consolidation stage. The fully clamped assembly was left to cure at room temperature for 24 hours.

3.6.4 Demolding and Post-processing

- Disassembly and Demolding: After 24 hours, the vice was opened and bolts were loosened. The mold side pieces were removed first, then the top cover taken off to extract the composite specimen. Demolding was performed carefully to avoid damaging delicate features.
- Post Processing of the Specimen: The extracted part underwent minor finishing operations: light deburring to remove flash and small resin burrs, followed by light sanding which was necessary to clean edges and critical surfaces. Sanding was minimal to preserve the intended geometry and surface features.

Figure 51 Demolded specimen.

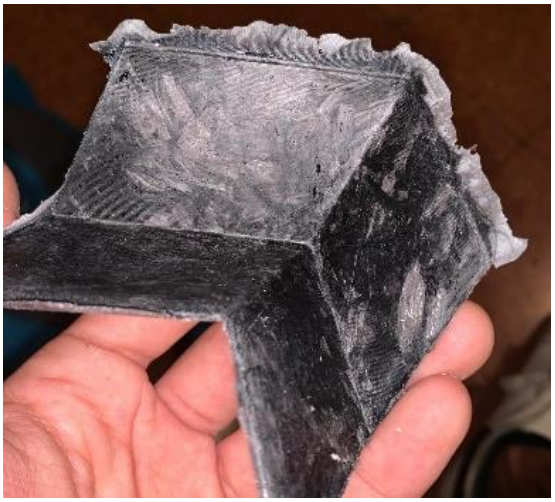

Figure 52 Unprocessed specimen.

Figure 53 Processed specimen.

Chapter 4

Results

4.1 Introduction

This chapter presents and discusses the results obtained from the experimental campaign described in the previous chapter 3. The objective of this phase was to evaluate the performance of the Forged Carbon Fiber manufacturing process, identify the main defects and limitations of the initial trials, and progressively optimize the parameters until achieving a defect-free and mechanically sound composite specimen.

Three successive manufacturing iterations were carried out, each aiming to address specific issues observed in the previous one. The first iteration served as a baseline to assess the quality of the initial process and identify defects such as voids, fiber gaps, and insufficient stiffness. The second and third iterations focused on refining the impregnation technique, adjusting the fiber-to-resin ratio, and improving the overall compaction of the material.

For each iteration, both visual and dimensional analysis were performed, supported by 3D scanning of the produced specimens to evaluate geometric accuracy and surface quality. These experimental observations are discussed in detail in the following sections, highlighting the progressive improvement of the manufacturing process and the elimination of the initial defects.

The scanner used in the laboratory is Roland Picza PIX-30 3D piezoelectric scanner, seen in Figure 54, using a needle to place points on the surface of the geometry. By placing these points, the software is able to map out the surface of the forged part on a high level of detail, where even small imperfections due to the accuracy of the fused deposition modelling on the mold and deformations due to the curing pressure and temperature can become apparent. Using the accompanying software of the scanner the level of accuracy can be selected and the size of the surface scanned. The scan is then exported in appropriate forms, so that it can be visualized.

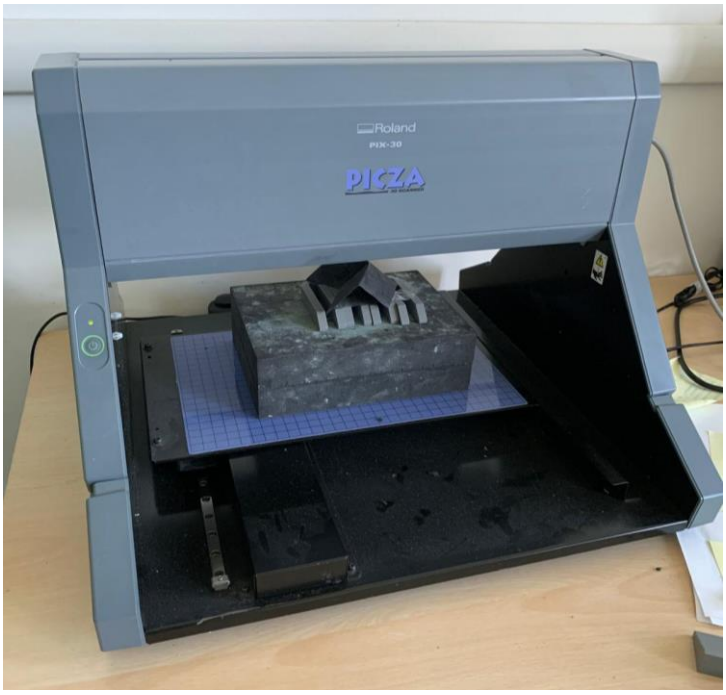

Figure 54 Roland Picza PIX-30 3D scanning a one-unit cell part.

Having a scan of a geometry, the user can visualize the point cloud and superimpose it against the initial geometry of the cylinder. In addition, after superposing the two geometries, it is also possible to derive the distance difference between points of the scan and the reference geometry, as will be seen in the following sections.

Subsequently, the mechanical properties of the optimized composite were evaluated through tensile testing. Finally, the scalability of the process was validated by producing a larger component consisting of four-unit cells, demonstrating the method's potential for future development and application in more complex geometries.

4.2 First Iteration: Prototype and Defect Analysis

The first iteration served as the baseline experiment to validate the overall manufacturing process and evaluate the behavior of the Forged Carbon Fiber during molding and curing. The objective was to verify the feasibility of producing the composite specimen using the 3D-printed ABS mold and to identify any defects or process limitations that would guide subsequent improvements.

The manufacturing procedure followed the methodology detailed in Chapter 3, including the impregnation of chopped carbon fiber tows with IN2 epoxy resin and AT30 fast hardener, followed by compression within the assembled mold and curing at room temperature for 24 hours. Once demolded, the part was subjected to both visual and dimensional inspections to assess its quality and conformity with the target geometry.

4.2.1 Visual Inspection

The surface of the specimen was carefully examined under both direct and transmitted light to identify visible defects. Three main issues were observed:

a) Void formation: A single void was detected on the lower surface, as seen in Figure 55, caused by the entrapment of an air bubble during the impregnation process.

b) Low rigidity: The specimen exhibited a slightly plastic-like feel and could be deformed under moderate pressure, suggesting inadequate stiffness meaning the fiber-to-resin ratio was not adequate.

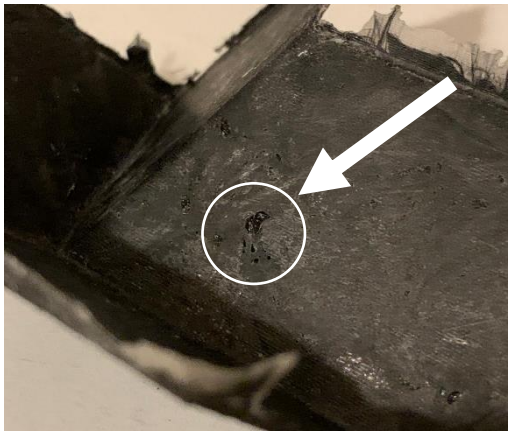

Figure 55 Void defect in first iteration.

c) Fiber gaps: When the part was held against a light source, small translucent regions were visible, as seen in Figure 56, indicating areas where the fiber packing density was insufficient or uneven, most likely because the compaction moved the fibers, which could affect the occlusion of the wave.

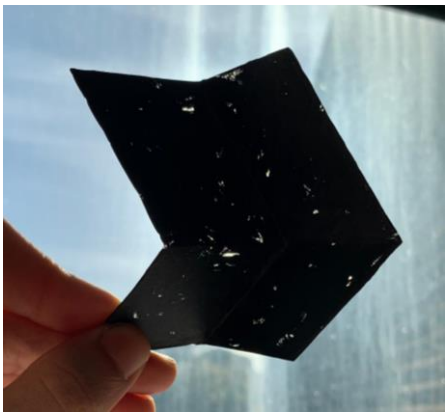

Figure 56 Fiber gaps in first iteration.

These observations indicated that, while the molding process was successful in producing the intended geometry, the impregnation and compaction parameters required optimization to improve both the structural and visual quality of the composite.

4.2.2 Dimensional Check

The thickness of the specimen was measured using a vernier caliper, confirming a nominal value of 1.0mm within acceptable tolerance at multiple locations across the surface, as shown in Figure 57.

Figure 57 Thickness measurement using a Vernier caliper.

To evaluate the surface quality and dimensional consistency, the 3D scanned model of the specimen was superposed onto the original CAD geometry. The resulting color-coded deviation map highlights the differences between the two surfaces, confirming that the mold semi-accurately reproduced the designed geometry, with only minor surface irregularities observed along the edges, as seen in Figure 58.

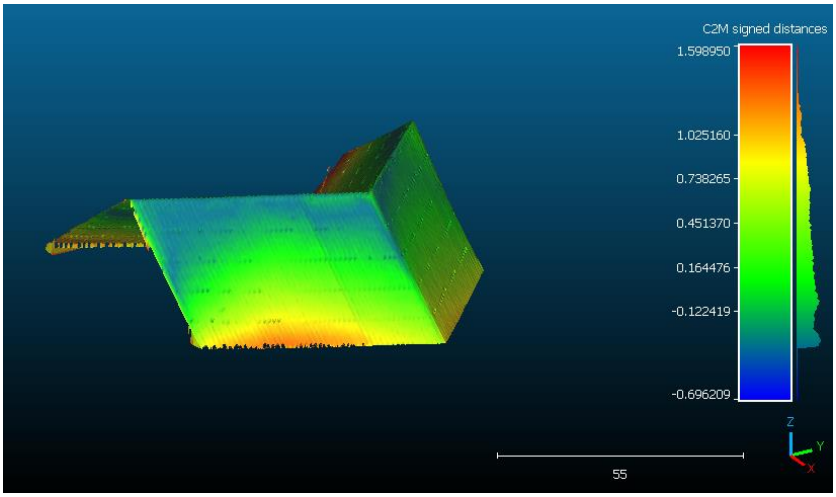

Figure 58 Color map of surface deviation between the 3D scan of the first iteration and the original CAD geometry.

The results of this first trial confirmed the feasibility of the process and the general reproducibility of the mold geometry but also highlighted the need for further improvements in geometric accuracy, resin impregnation control, fiber distribution, and compaction. The modifications introduced to address these limitations are discussed in the following sections.

4.3 Second Iteration: Process Refinement

Following the identification of voids, fiber gaps, and low rigidity in the first prototype, a second iteration was conducted to improve both the internal structure and the mechanical feel of the composite specimen. The objective of this iteration was to enhance resin impregnation, increase compaction during molding, and adjust the fiber-to-resin ratio to achieve a denser and more cohesive material.

4.3.1 Process Adjustment

During the impregnation phase, greater care was taken in manually applying the resin to the chopped carbon fibers using the brush. The process was slowed down to allow for more uniform resin distribution and to ensure complete wetting of the fibers, thereby minimizing the risk of trapped air or dry spots; also, to make sure that no air bubbles were formed, a torch was passed all over the area to pop all the bubbles.

Additionally, the vice was tightened more firmly during the compression phase to promote improved resin drainage and higher fiber compaction inside the mold cavity.

The fiber-to-resin ratio was modified from 60:40 to 50:50 by weight. This adjustment was made to provide a better balance between stiffness and resin bonding, increasing the overall structural cohesion of the specimen.

4.3.2 Results and Observations

The resulting specimen demonstrated clear improvements in mechanical behavior and appearance compared to the first iteration. The void previously observed on the lower surface was completely eliminated, confirming that the improved impregnation and higher compression pressure were effective.

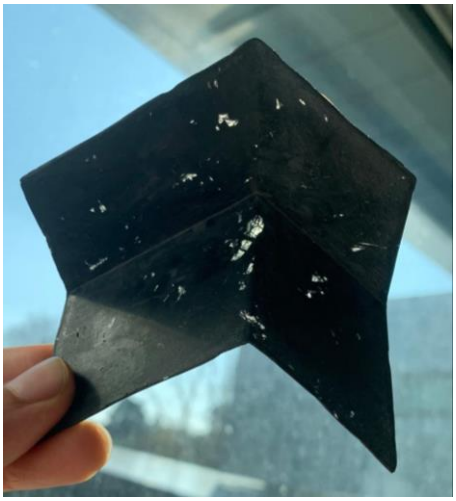

Figure 59 Fiber gaps in second iteration.

The part also exhibited greater stiffness and rigidity, with a more solid tactile feel, indicating a denser material structure. However, when examined under transmitted light, as seen in Figure 59, fiber gaps remained visible, suggesting that while compaction and wetting had improved, the fiber packing density was still not completely uniform, with some localized regions showing lower fiber concentration.

4.3.3 Dimensional Analysis

A 3D scan was again performed to verify geometric accuracy and detect any potential deformation induced by the higher compression pressure. The scan was superposed onto the CAD model, and the results showed even better alignment compared to the previous iteration. The geometry closely matched the intended design, as seen in Figure 60, with noticeably reduced deviations along the edges, confirming that the increased compaction pressure further improved dimensional accuracy without introducing distortion.

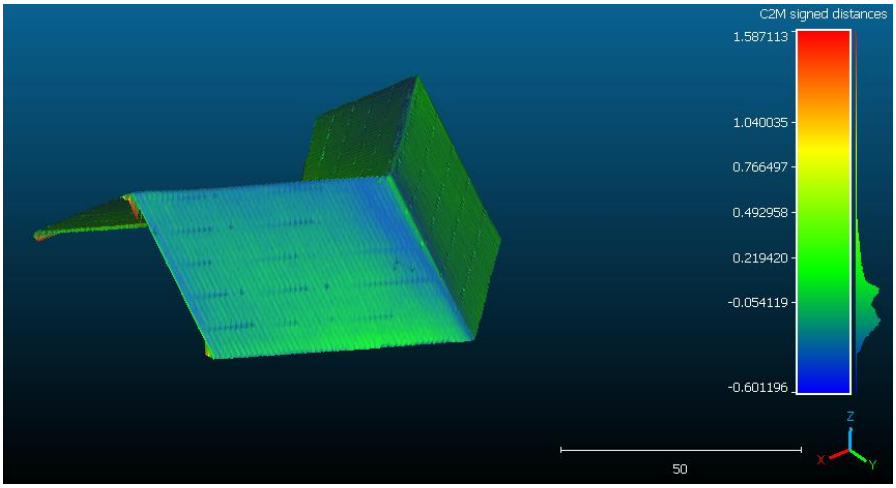

Figure 60 Color map of surface deviation between the 3D scan of the second iteration and the original CAD geometry.

Overall, the second iteration successfully demonstrated that improved resin impregnation and higher clamping pressure could eliminate voids and enhance stiffness. However, the persistence of localized fiber gaps indicated that further optimization was still required. These refinements were introduced in the third iteration, described in the following section.

4.4 Third Iteration: Optimized Process

The third iteration was performed with the objective of completely eliminating the remaining fiber gaps and achieving a denser, defect-free, and mechanically robust specimen. Based on the observations from the previous trials, this experiment focused on increasing the total mass of the materials used while maintaining the optimal fiber-to-resin ratio determined in the second iteration.

4.4.1 Process Adjustments

In this iteration, the fiber-to-resin ratio was maintained at 50:50 by weight, as it had previously shown a good balance between stiffness and resin bonding. However, the total calculated mass was modified to further increase fiber compaction and ensure complete mold filling.

Instead of determining the total weight as volume multiplied by 1.4 (as suggested by the manufacturer), the mass was doubled by a factor of 2 relative to the

mold cavity volume. This adjustment resulted in 5g of fiber and 5g of resin, with an additional 40% excess resin prepared to compensate for expected drainage and losses during brushing and impregnation.

The impregnation technique and compression steps followed the same procedure as before, ensuring careful fiber wetting and progressive tightening of the vice. The increased material quantity was expected to promote higher internal pressure during compression, leading to improved fiber packing density and reduced internal voids.

4.4.2 Results and Observations

The resulting specimen showed a significant improvement in overall quality compared to previous iterations, seen in Figure 61.

- No voids were observed on any surface, confirming a complete resin impregnation.
- The fiber gaps visible in earlier specimens were entirely eliminated, even when examined under transmitted light.
- The part exhibited a notably higher stiffness and a solid, compact feel, indicating a well-bonded internal structure.

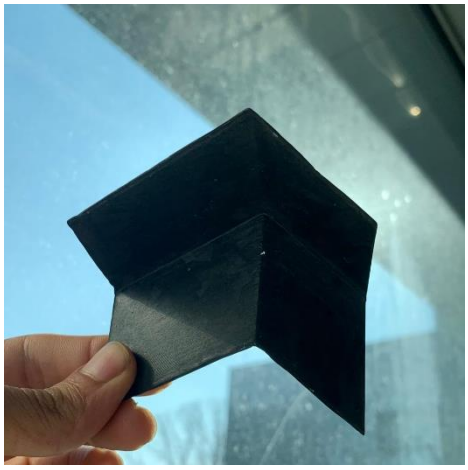

Figure 61 Fiber gaps in third iteration.

The surface finish was also improved, showing a more uniform texture with minimal resin-rich zones. These results confirmed that the combination of increased total mass and careful impregnation provided the optimal balance between fiber compaction, resin flow, and drainage.

4.4.3 Dimensional Analysis

A 3D scan of the third specimen was conducted and superposed onto the reference CAD geometry to verify dimensional accuracy. The analysis demonstrated an almost perfect correspondence between the scanned geometry and the original CAD model. The surface appeared uniformly green in the deviation map, indicating minimal dimensional variation and confirming that this iteration achieved the highest geometric accuracy among all trials. The geometry was faithfully reproduced, with negligible deviations even along the edges, verifying that the increased mass and higher compaction pressure resulted in optimal dimensional stability.

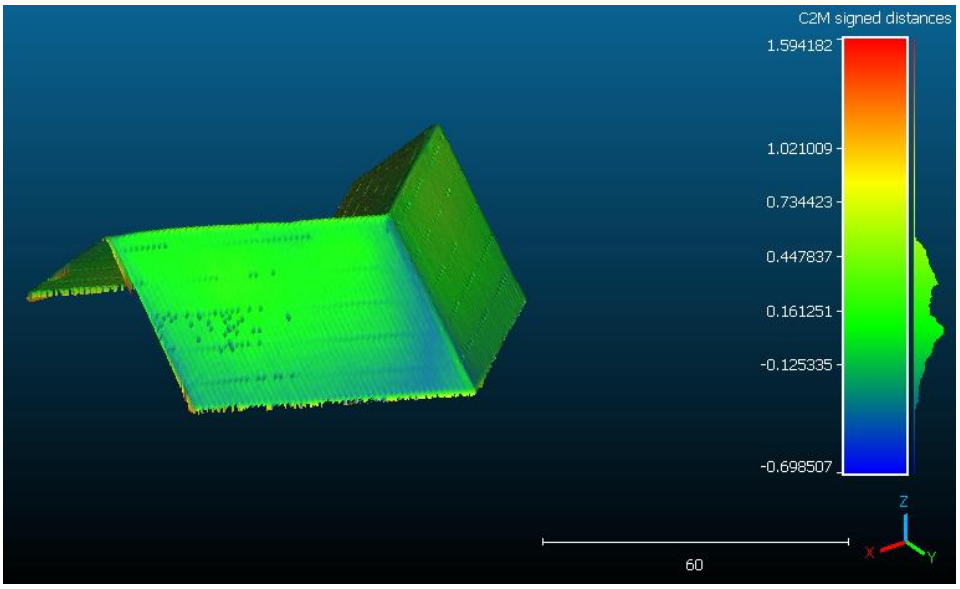

Figure 62 Color map of surface deviation between the 3D scan of the third iteration and the original CAD geometry.

This third iteration successfully produced a defect-free and dimensionally accurate composite specimen, representing the optimized configuration for this manufacturing process. The parameters and material proportions determined in this phase were therefore adopted as the reference for the subsequent mechanical testing and scalability study, presented in the following sections.

4.5 Mechanical Testing Results

4.5.1 Introduction to the Test

The tensile test was performed to evaluate the mechanical behavior of the optimized Forged Carbon Fiber composite and to establish a reference for its structural performance. Although the primary function of the metamaterial developed in this thesis is acoustic attenuation, any component intended for potential aerospace applications must satisfy minimum standards of mechanical integrity. For this reason, the tensile test provides essential baseline data on the stiffness, strength, and failure characteristics of the composite.

To contextualize these results, the composite specimen was compared to Aluminum 5154-H36, a conventional lightweight alloy commonly used in structural applications. The objective of this comparison is not to match the performance of aluminum, but rather to establish a mechanical baseline, illustrating how the Forged Carbon Fiber composite behaves relative to a well-characterized engineering material. The aluminum specimens were manufactured using waterjet cutting, ensuring dimensional accuracy and eliminating thermal distortion, thereby providing a reliable benchmark for comparison.

The composite tensile specimens were designed and fabricated specifically for this study, following the same molding approach used in producing the metamaterial unit cell. This ensured that the fiber distribution, resin content, and curing conditions in the tensile coupons accurately represent the internal structure of the final component. Prepared in accordance with ASTM D3039/D3039M, with minor deviations in specimen geometry. The specimens were manufactured with a total length of 200 mm, gauge length of 85 mm, gauge width of 13 mm, and thickness of 5 mm due to material and manufacturing constraints. [38]

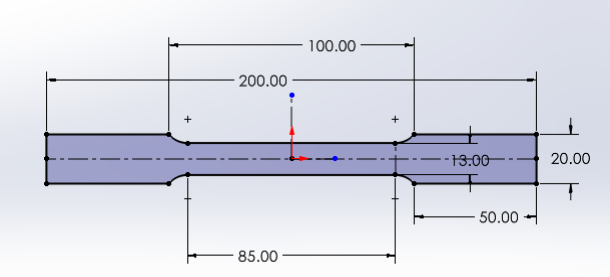

Figure 63 Design sketch of the specimen.

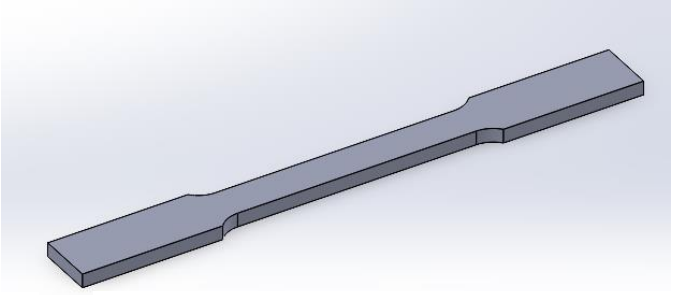

Figure 64 Specimen preview.

To ensure statistical validity and compliance with ASTM recommendations, three specimens were tested for each material—three for the Forged Carbon Fiber composite and three for the Aluminum 5154-H36 alloy. All tests were conducted using the standard universal tensile testing machine available in the University of Bologna laboratories, manufactured by ITALSIGMA s.r.l [39]. An extensometer was mounted on each specimen to accurately measure strain in the gauge length, ensuring reliable determination of the elastic modulus and other strain-dependent properties.

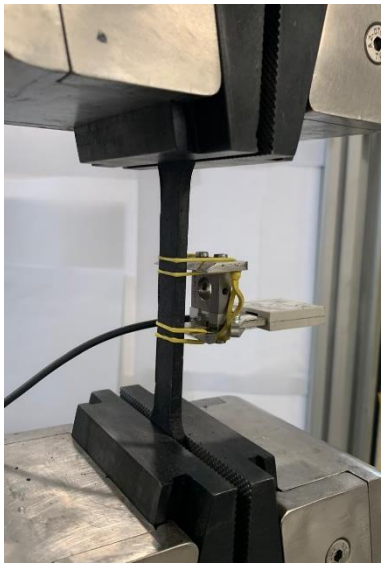

Figure 65 Tensile test setup.

Figure 66 ITALSIGMA tensile testing machine.

4.5.2 Stress-Strain Curves

The tensile behavior of both the Forged Carbon Fiber composite and the Aluminum 5154-H36 specimens was evaluated by examining their corresponding stress–strain curves. For each material, the three individual curves obtained from the repeated tests were plotted and compared to assess consistency and repeatability. Since the results of the real test were noisy, a smoothened curve was also made to make it easier to read.

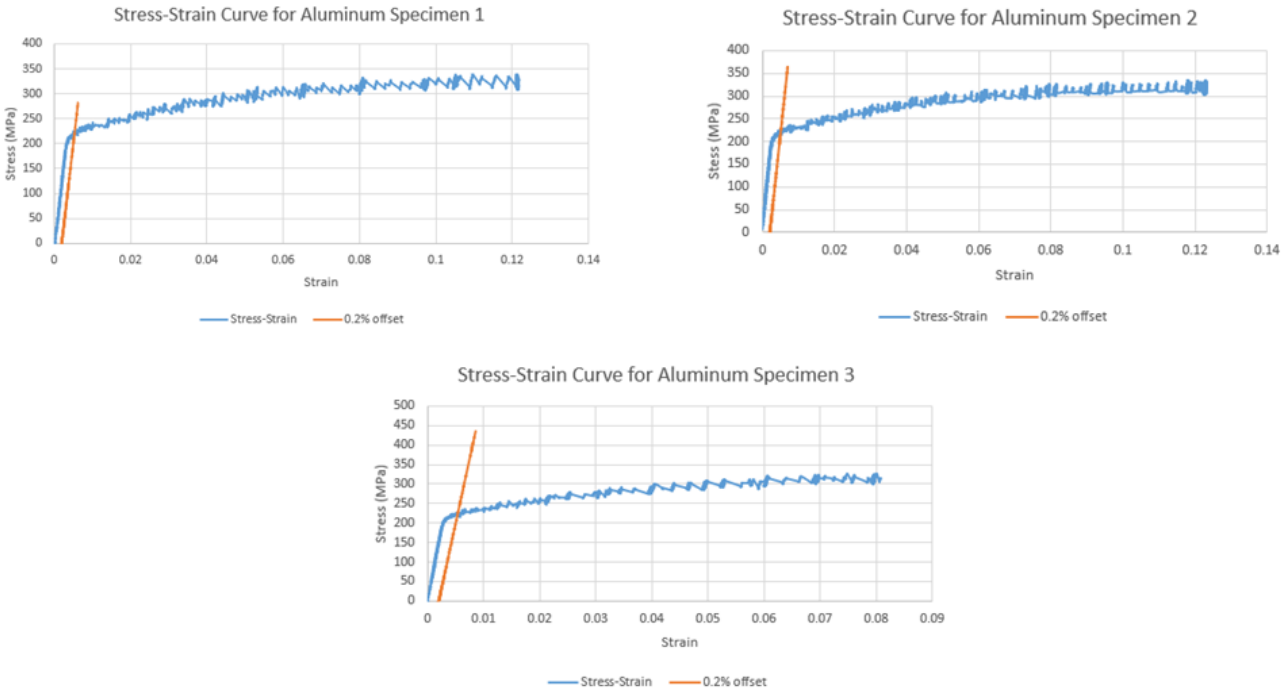

Figure 67 Stress-Strain curves of Aluminum specimens.

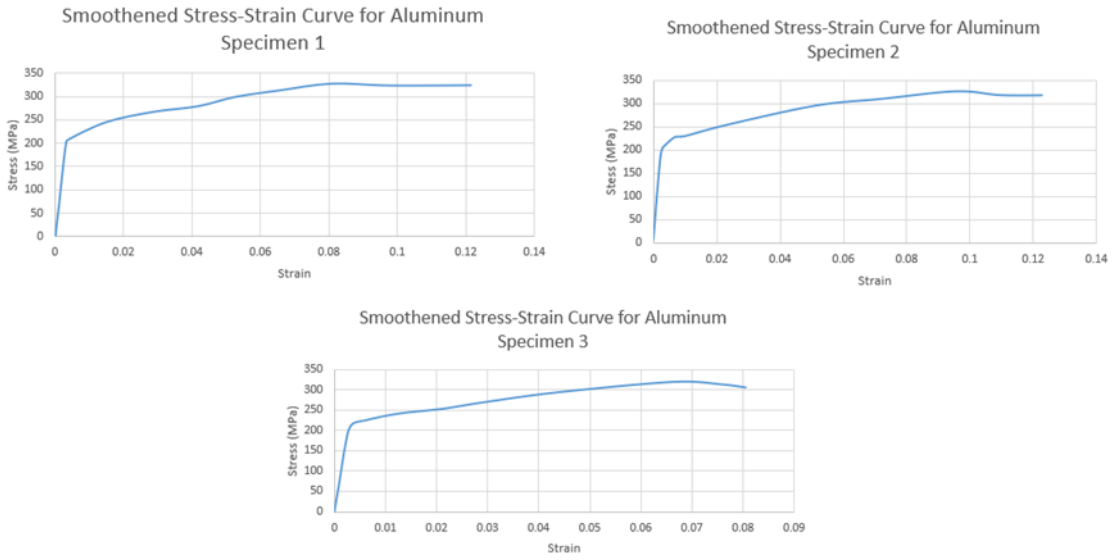

Figure 68 Smoothened Stress-Strain curves of Aluminum specimens.

The Aluminum specimens displayed the expected ductile behavior of a strain-hardened aluminum alloy. After the initial linear elastic region, the curve instantly went to the strain hardening region prior to reaching an ultimate strength point and then it went to failure. From these curves we can get a lot of values that quantify some mechanical properties of this material.

Table 5 Mechanical properties of tested Aluminum specimens.

	Specimen 1	Specimen 2	Specimen 3	Mean
Youngs Modulus E (GPa)	66	73.5	66.4	68.63
Yield Strength (MPa)	221.53	219.3	222.46	241.1
Ultimate Tensile Strength (MPa)	326.4	326.7	320.15	324.41
Stress at Failure (MPa)	322.9	316.6	314.76	318.08
Elongation at Break	12% (10.2mm)	12.2% (10.37mm)	8% (6.8mm)	10.73

The mechanical properties extracted from the stress–strain curves of the Aluminum 5154-H36 specimens are fully consistent with the typical behavior of a strain-hardened aluminum alloy. The material exhibits a well-defined elastic region, followed by a noticeable yield point, and then a region of work hardening before failure. This confirms the expected ductile response, characterized by significant plastic deformation prior to fracture.

The measured properties—namely the elastic modulus, yield strength, ultimate tensile strength, and elongation at break—serve primarily as a benchmark dataset. Aluminum 5154-H36 was selected for this purpose because it represents a well-established engineering material with predictable and widely documented mechanical performance. By testing aluminum specimens designed with the same geometry and under the same testing conditions, it becomes possible to establish a reliable reference against which the behavior of the Forged Carbon Fiber composite can be meaningfully compared. This baseline allows us to evaluate how the composite performs not only in terms of absolute strength and stiffness, but also in relation to a conventional lightweight structural material.

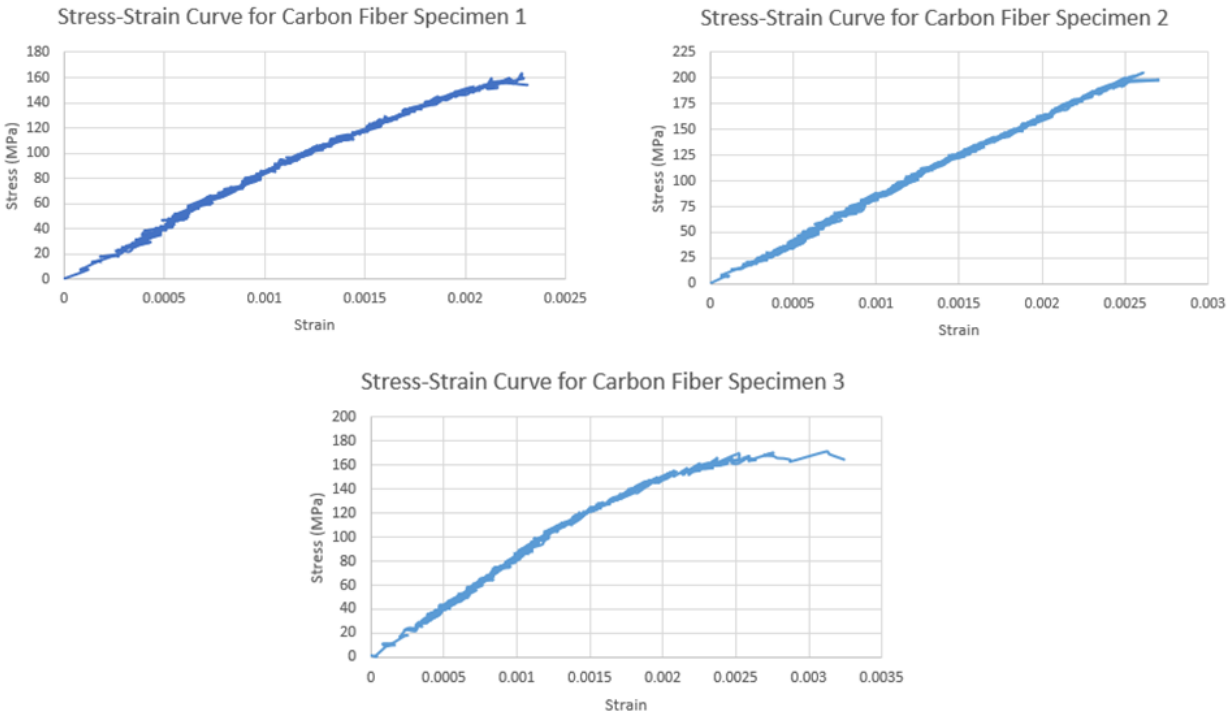

Figure 69 Stress-Strain curves for carbon fiber specimens.

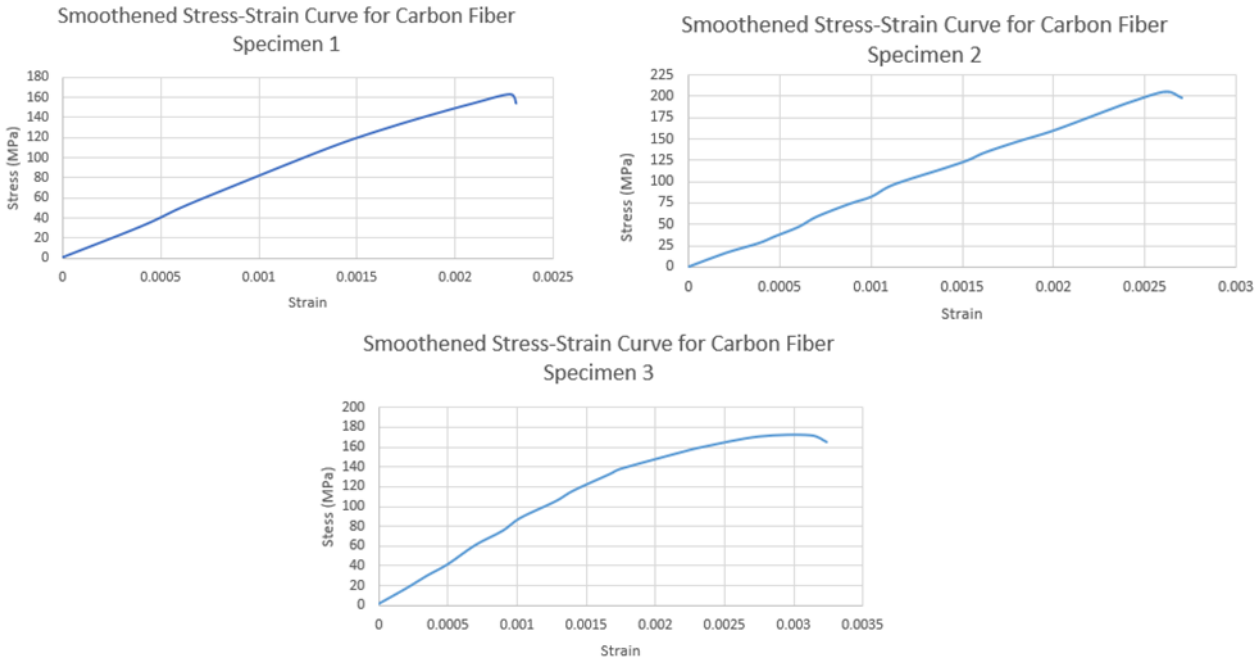

Figure 70 Smoothened Stress-Strain curves for carbon fiber specimens.

Table 6 Mechanical properties of tested carbon fiber specimens.

	Specimen 1	Specimen 2	Specimen 3	Mean
Tensile Stiffness E (GPa)	74.3	81.1	78.7	78.03
Yield Strength (MPa)	-	-	-	-
Ultimate Tensile Strength (MPa)	163.07	205.23	171.54	179.94
Strain at Failure	0.00231	0.0027	0.0032	0.0027
Elongation at Break	-	-	-	

The stress–strain curves obtained from the three Forged Carbon Fiber specimens exhibit a consistent overall trend that is characteristic of chopped fiber–reinforced polymer composites. All three curves show a predominantly linear elastic response, indicating that the material behaves elastically up to failure with minimal plastic deformation. The slope of the initial linear region reflects the stiffness of the composite, and although minor variations appear between specimens, the general shape remains similar, confirming good repeatability of the manufacturing process. As strain increases, each specimen reaches a distinct maximum tensile stress, after which a sudden drop is observed, corresponding to a brittle fracture typical of short carbon fiber systems. Differences in peak stress and ultimate strain among the three specimens can be attributed to slight variations in fiber packing density, fiber orientation randomness, and microstructural heterogeneity inherent to the forged composite process.

Visual inspection of the fractured surfaces showed resin-dominated breakage, indicating that failure was governed by interfacial debonding rather than fiber rupture, as seen in Figure 71. This is consistent with the manufacturing process, where fibers were placed in a random orientation and resin-impregnated manually.

Figure 71 Fracture in the tensile specimen.

4.5.3 Comparison Between Aluminum and Forged Carbon Fiber Specimens

To contextualize the performance of the forged composite, the results were compared to the aluminum baseline specimens produced under identical testing conditions. The aluminum samples serve solely as a reference material, enabling consistent comparison of mechanical behavior using specimens with identical geometry, the same testing machine, and the same extensometer setup.

When comparing the two materials, the forged carbon fiber specimens exhibited significantly higher stiffness than the aluminum, despite being produced from thin and discontinuous fibers. The carbon fiber elastic moduli (ranging approximately between 74–81GPa) were consistently greater than those of the aluminum benchmark specimens. This demonstrates that even with a non-continuous fiber distribution, the composite retained a high modulus characteristic of carbon-based reinforcements.

In terms of ultimate tensile strength, the aluminum samples outperformed the composite, reaching values above 320MPa, whereas the forged carbon fiber specimens fell within the 160-205MPa range. This is expected, given that the forged composite relies on randomly oriented chopped fibers and a resin matrix, whereas the aluminum behaves as a homogeneous, ductile metal. The forged composite's failure was brittle and abrupt, while aluminum showed extensive ductility with elongation exceeding 8–12%, highlighting the contrasting failure mechanisms.

Despite the lower strength, the forged composite's high stiffness-to-weight ratio, brittle tensile response, and lightweight nature offer clear advantages for applications where mass reduction and vibrational/noise attenuation are prioritized. Importantly, this comparison establishes a quantitative frame of reference showing that the forged composite provides sufficient stiffness and structural integrity for the intended metamaterial application, demonstrating that the final component is capable of withstanding the mechanical loads expected in an aircraft environment, despite being optimized primarily for noise-attenuation performance.

4.6 Scalability and Final Demonstration

A core requirement for the adopted metamaterial concept is its ability to scale from a single unit cell to multi-cell configurations while preserving geometry, structural integrity, and manufacturability. To assess this, the manufacturing procedure validated in the third iteration was applied to produce a larger specimen composed of four-unit cells, using the same mold design logic, fiber-to-resin ratio, impregnation steps, and compression protocol.

The mold for this final component followed the same design process as the original ABS mold. However, due to temporary unavailability of the Fortus printer, the final mold was manufactured using PETG rather than ABS. From a functional standpoint, this substitution did not introduce any noticeable differences: PETG provided sufficient dimensional stability, thermal resistance, and surface quality for the forging process, allowing the experiment to proceed under equivalent conditions.

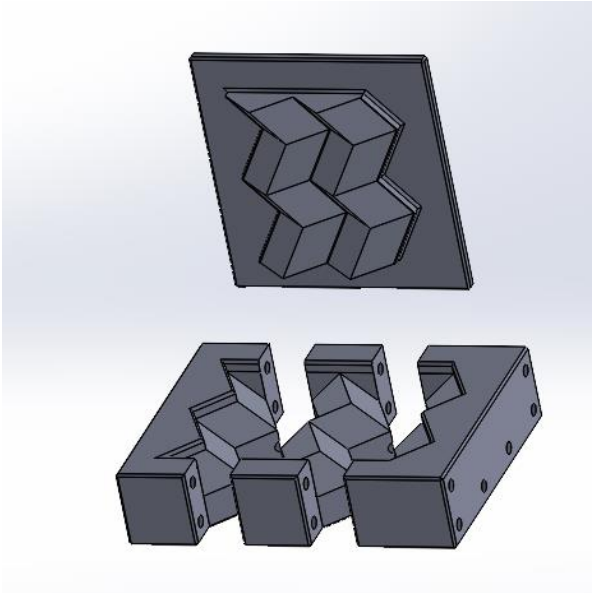

Figure 72 Mold design for 4 unit-cells component.

The four-cell mold seen in Figure 72 was generated by scaling and extending the original CAD geometry while maintaining the same wall thicknesses, hinge features, and cavity constraints required by the metamaterial design, the only major difference is the addition of a new center piece to facilitate the demolding process . The forging procedure was executed using the same fiber-to-resin ratio, impregnation sequence, and compression approach established in the third single-cell iteration.

The resulting four-unit-cell component was successfully manufactured and reproduced the expected global geometry. Nonetheless, two minor defects were observed:

- One small void appeared on the surface, caused by trapped air bubbles during resin application. This void is superficial and can be easily corrected by applying small drops of resin, meaning it doesn't represent a failure of the process.

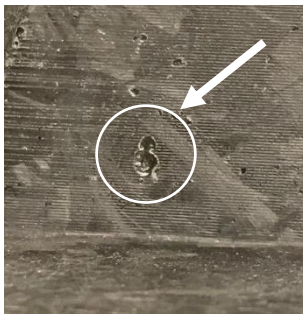

Figure 73 Void present on the 4 unit-cells component.

- Light fiber gaps were visible when the part was illuminated from behind. This phenomenon is attributed to the larger compressed area: distributing the clamping pressure uniformly across a bigger mold surface is more challenging, allowing slight fiber movement before gelation. While these gaps do not compromise the structural performance of the specimen, they highlight an area for improvement in pressure distribution—potentially through upgraded clamping.

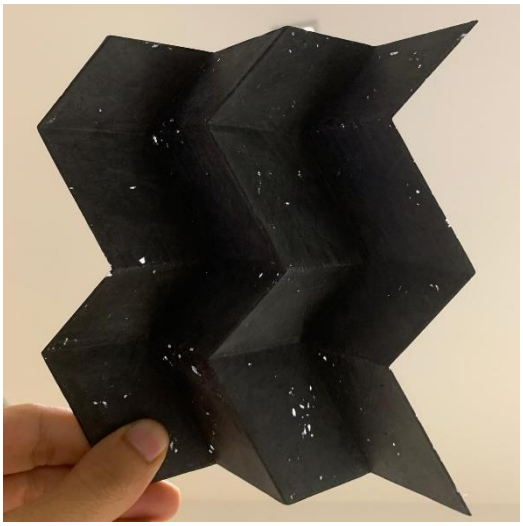

Figure 74 Fiber gaps present in the 4 unit-cells component.

Despite these minor imperfections, the successful fabrication of the four-unit specimen demonstrates that the process is scalable and that both the composite formulation and the 3D-printed mold approach can be extended to larger geometries. The geometry remained consistent, the surface quality was acceptable, and the structural integrity matched expectations for short-fiber thermoset composites.

This achievement confirms that the proposed manufacturing strategy can be used to create larger metamaterial assemblies which is an essential requirement for their practical application in aerospace noise-reduction structures. Visual documentation of the final specimen is presented in Figure 75.

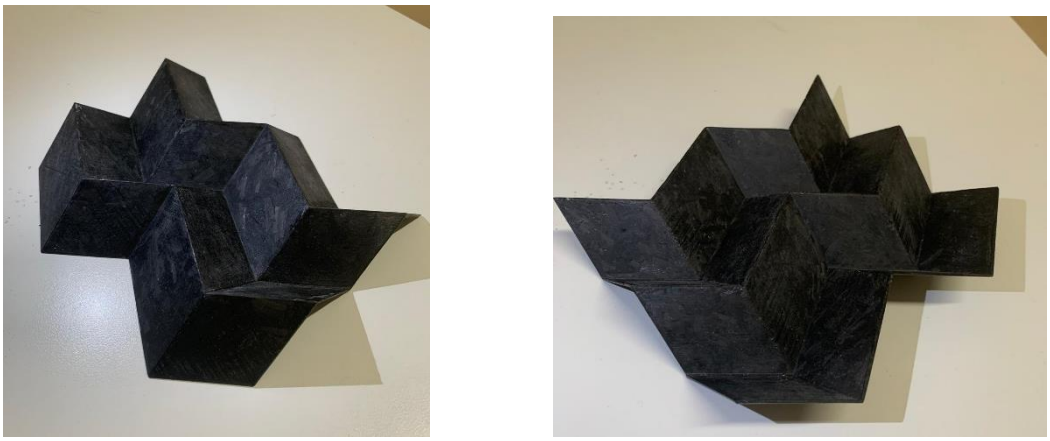

(a) (b)

Figure 75 Final 4 unit-cells component from
(a) top view / (b) bottom view.

4.7 Summary

This chapter presented the comprehensive experimental and analytical evaluation of the forged carbon-fiber metamaterial specimens and their progression from initial prototypes to a scalable multi–unit-cell configuration. The first section reported the results of the initial single-cell experiment, including visual inspection, dimensional verification through 3D scanning, and identification of early defects such as void formation, fiber gaps, and insufficient stiffness. These observations guided the refinement of the manufacturing process.

Subsequent sections detailed the second and third iterations, where improvements in resin impregnation, clamping pressure, and fiber-to-resin ratio successfully eliminated voids and reduced fiber gaps, ultimately yielding a single-unit specimen with consistent geometry, stronger mechanical behavior, and acceptable surface quality. Tensile testing of the optimized composite was then performed and benchmarked against aluminum specimens prepared under identical conditions. The results confirmed that the forged composite met the required performance for metamaterial applications, providing sufficient strength and stiffness despite its chopped-fiber microstructure.

Finally, the chapter demonstrated the scalability of the process by manufacturing a four-unit-cell component using the optimized parameters. The larger part reproduced the intended geometry and structural characteristics, with only minor defects attributable to the increased compression area. This successful scale-up validated the feasibility of extending the manufacturing approach to more complex and larger metamaterial configurations—an essential requirement for practical aerospace applications.

Conclusion

This thesis investigated the feasibility of manufacturing an origami-inspired metamaterial through a sheet-molding-compound (SMC) approach that combines forged chopped carbon fibers with low-cost, additively manufactured molds. The objective was to develop a manufacturing strategy capable of reproducing complex folded geometries—unachievable by conventional composite lay-up—while ensuring that the resulting composite could withstand the moderate mechanical loads required for lightweight aerospace applications, particularly where noise attenuation and structural integrity must coexist.

A complete design-to-fabrication workflow was developed, beginning with the CAD modeling of a single unit cell. The geometric requirements of the origami-based metamaterial demanded a mold capable of producing sharp folds, thin structural features, and precise internal angles. Multi-part molds were designed accordingly and fabricated using FDM 3D printing. The material selection strategy addressed both composite and tooling needs: chopped 6K carbon fibers and a low-temperature-curing IN2/AT30 epoxy system for the composite, and ABSplus P430—or PETG for the final scaled test—provided adequate thermal stability and dimensional accuracy for mold construction.

The experimental manufacturing process evolved across three iterations. The first specimen revealed voids, insufficient compaction, fiber gaps, and a softer-than-desired feel due to low fiber content. These defects guided refinements that included more careful resin impregnation, higher clamping force, and adjustment of the fiber-to-resin ratio. By the third iteration, the process consistently produced specimens with uniform thickness, improved stiffness, and minimal defects, demonstrating the effectiveness and reproducibility of the method.

Mechanical testing provided quantitative support for these results. Tensile specimens manufactured using the optimized process exhibited a linear elastic response followed by brittle failure, characteristic of chopped-fiber composites. Benchmarking against Aluminum 5154-H36 under identical conditions established a useful reference, showing that the forged composite offered adequate stiffness and load-bearing behavior for non-primary aerospace applications such as acoustic inserts or lightweight interior structures.

A major achievement of this research was the demonstration of scalability. Using the refined process, a four-unit-cell component was successfully manufactured, validating the ability of the system to handle more complex and larger geometries. Minor imperfections—small voids and slight fiber gaps—were attributed to pressure distribution challenges over the larger mold area, not to limitations in materials or process fundamentals. The ability to scale from one-unit cell to a four-unit configuration confirms that further expansion to even larger metamaterial assemblies is feasible.

Overall, the findings of this thesis show that forged SMC composites, combined with 3D-printed polymer molds, represent a robust, low-cost, and versatile manufacturing route for origami-inspired metamaterials. The approach enables rapid iteration, geometric customization, and reliable replication of complex folding patterns, while providing the structural performance necessary for practical engineering use.

Looking forward, several opportunities for advancement emerge naturally from this study. One of the most promising is the incorporation of long, unimpregnated continuous fibers placed strategically within the forged structure. By aligning these reinforcements along known load paths, the material could develop controlled anisotropy, significantly increasing stiffness and strength in targeted directions while the surrounding chopped-fiber matrix maintains formability and acoustic performance. Such hybridization could bridge the gap between high-performance laminates and isotropic SMC materials.

Further improvements could focus on enhancing pressure distribution during compression of larger components, potentially through redesigned clamping systems or distributed load fixtures to eliminate fiber migration and ensure more uniform compaction. Additionally, exploring alternative mold materials or surface coatings may improve durability, thermal stability, and surface finish. Since noise attenuation is the primary functional goal of the metamaterial, future work should also include dedicated acoustic performance testing to quantify the frequency-dependent benefits of the geometry and material system. Finally, extended mechanical qualification—fatigue, impact, and environmental conditioning—would be necessary steps toward evaluating the material's suitability for regulated aerospace environments.

In summary, this thesis demonstrates that SMC-based forging using 3D-printed molds is a practical and scalable method for producing origami-inspired metamaterials, offering a compelling combination of design flexibility,

manufacturability, and mechanical performance. The work provides a strong foundation for future development of lightweight, functionally tailored acoustic metamaterials for aerospace and other advanced applications.

Bibliography

[1] ASTM, "Standard Terminology for Additive Manufacturing – General Principles – Terminology," *ASTM International,* no. 52900, pp. 1-2, 2015.

[2] J. Hiemenz, "3D printing with FDM: How it Works," *Stratasys Inc,* vol. 1, pp. 1-5, 2011.

[3] A. Kashani, G. Imbalzano, K. Nguyen and D. Hui, "Additive manufacturing (3D printing): a review of materials, methods, applications and challenges," *Compos. B Eng,* no. 143, pp. 172-196, 2018.

[4] M. Zimmers and E. Groover, "CAD/CAM: computer-aided design and manufacturing," *Pearson Education,* 1983.

[5] S. Fletcher, "The rapid prototyping technologies," *Assembly,* no. 23.4, p. 318–330, 2003.

[6] E. Hutzell, "Slicing and 3D Printing File Types Overview," *University of Maryland ,* vol. 1, pp. 1-6.

[7] K. Hernandez and A. Wong, "review of additive manufacturing," *Wiley Online Library,* vol. 2012, p. 208760, 2012.

[8] Z. Wang, W. Hao, W. Hongtao, C. John, R. Qifeng, L. Hailong and k. Joel, "2.5D, 3D and 4D printing in nanophotonics - a progress report," *Materials Today: Proceedings,* vol. 70, pp. 304-309, 2022.

[9] T. Wohlers, "Additive Manufacturing Advances," *Manufacturing Engineering,* vol. 148, no. 4, pp. 55-56, 2012.

[10] W. T, "Wohlers Report 2010," Wholers Associates, 2010.

[11] A. Equbal, "Rapid tooling: A major shift in tooling practice," *Manufacturing and Industrial Engineering,* vol. 14, pp. 3-4, 2015.

[12] S. Cecchel and G. Cornacchia, "Additive manufacturing for rapid sand casting: mechanical and microstructural investigation of aluminum alloy automotive prototypes," *Metals,* vol. 14, no. 4, p. 459, 2024.

[13] H. Yang, Z. Shan, D. Yan, J. Shi and Q. Liu, "Research on forming method of additive manufacturing of frozen sand mold," *Heliyon,* vol. 9, no. 8, 2023.

[14] G. Kim, E. Barocio, W. Tsutsui, P. Wang, S. Dubikovsky, R. Pipes and R. Sterkenburg, "Applicability assessment of thermoset coating onto additively manufactured thermoplastic composite molds," *Additive Manufacturing,* vol. 61, p. 103289, 2023.

[15] A. Hassen, E. Betters, N. Tsiamis, J. West, T. Smith, K. Billah, D. Nuttall, V. Kumar, S. Smith and V. Kunc, "Joining technique for in-oven/autoclave molds manufactured by large scale polymer additive manufacturing," *Manufacturing Letters,* vol. 32, pp. 77-82, 2022.

[16] Q. Jia, B. Liu, S. Li, C. Hu, Y. Yang and G. Wang, "Slurry-based photoinitiator jetting process for ceramic additive manufacturing," *Additive Manufacturing,* vol. 86, p. 104185, 2024.

[17] M. Thomas, M. Cynthia, Gomes, H. Jürgen and G. Jens, "Slurry-Based Additive Manufacturing of Ceramics," *Applied Ceramic Technology,* vol. 12, no. 1, pp. 18-25, 2015.

[18] P. Kruth, "Material incress manufacturing by rapid prototyping techniques," *CIRP Annals—Manufacturing Technology,* vol. 2, no. 40, p. 603–614, 1991.

[19] S. Mohamed, J. Abby and R. James, "3D-Printed Biosensor Arrays for Medical Diagnostics," *Micromachines,* vol. 9, 2018.

[20] S. E. Gunaslan, A. Karasin and M. Öncü, "Properties of FRP Materials," 2014.

[21] F. C. J. Campbell, "Manufacturing Technology for Aerospace Structural Materials," *Elsevier,* 2011.

[22] S. Sharma, L. Sowntharya and K. Kar, "Polymer-Based Composite," *Composite Materials: Processing, Application, Characterizations,* pp. 1-36, 2017.

[23] F. Campbell, "Structural Composite Materials," *ASM International,* vol. 14, 2010.

[24] R. M. Jones, "Mechanics of composite materials," *CRC press,* 1999.

[25] H. Marks and Q. Pham, "Epoxy resins," *Ullmann's Encyclopedia of,* 2000.

[26] C. K., "Glass transition temperature (Tg) - A210.," *Practice Centre,* 2021.

[27] "EasyComposites," EasyComposites, [Online]. Available: https://www.easycomposites.eu/forged-carbon-fibre-kit.

[28] Alghamdi and Choudhury N, "Additive manufacturing of polymer materials: progress, promise and challenges," *Polymers,* vol. 13, p. 1–39, 2021.

[29] C. Khoe, R. Sen and V. Bhethanabotla, "Oxygen Permeability of Fiber-Reinforced Polymers," *Composites for Construction,* vol. 15, pp. 513-521, 2011.

[30] "Easycomposites," Easycomposites, [Online]. Available: https://www.easycomposites.co.uk/learning/mechanical-properties-of-forged-carbon-fibre.

[31] D. Systemes, "Solidworks. 2019," *Dassault Systemes: Vélizy - Villacoublay,* p. 434, 2019.

[32] D. Rypl and Z. Bittnar, "Generation of computational surface meshes of STL models," *Journal of Computational and Applied Mathematics,* vol. 192, no. 1, pp. 148-151, 2006.

[33] "FDM Systems and Materials Overview - EN Brochure," Stratasys, 2024. [Online]. Available: https://support.stratasys.com/en/Printers/FDM-Legacy/Fortus-250mc.

[34] Stratasys, "Stratasys," Strasasys, [Online]. Available: https://support.stratasys.com/it/materials/fdm/absplus-p430.

[35] C. Maria, F. Matteo, P. Vasilena, M. Martino C, P. Marco and P. Giuseppe, "Vibro acoustic characterization of aerospace structures made of Miura-Ori origami metamaterial," University of Bologna, Bologna, 2024.

[36] K. Tanizawa and K. Miura, "Large displacement configurations of bi-axially compressed infinite plate," *Trans Jpn Soc Aeronaut Space Sci,* vol. 20, no. 50, pp. 177-187, 1978.

[37] Toray, "TorayCA," Toray, [Online]. Available: www.toraycma.com.

[38] ASTM, "StandardTest Method for Tensile Properties of Polymer Matrix Composite Materials," *ASTM International,* pp. 1-13, 2014.

[39] "italsigma.it," ITALSIGMA S.R.L., 2019. [Online]. Available: https://www.italsigma.it/macchine/macchine-oleodinamiche/.